AD-A110 892 MASSACHUSETTS INST OF TECH CAMBRIDGE F/G 7/4
ELECTROCHEMICAL STATE MODELS OF LEAD-ACID BATTERIES.(U)
MAY 79 R J PFISTER

UNCLASSIFIED NL

1 OF 2
AD A
110892

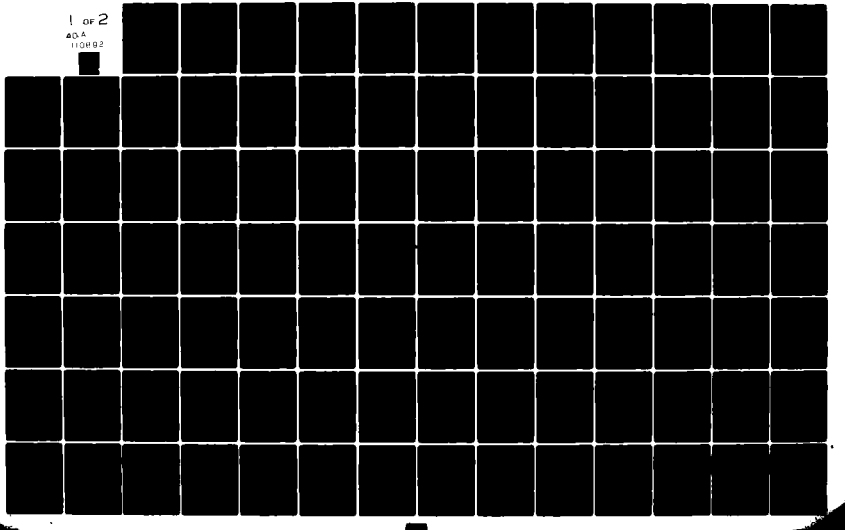

UNCLASS

SECURITY CLASSIFICATION OF THIS PAGE (When Data Entered)

REPORT DOCUMENTATION PAGE	READ INSTRUCTIONS BEFORE COMPLETING FORM
1. REPORT NUMBER / 2. GOVT ACCESSION NO.	3. RECIPIENT'S CATALOG NUMBER
4. TITLE (and Subtitle): Electrochemical State Models of Lead-Acid Batteries	5. TYPE OF REPORT & PERIOD COVERED: THESIS
	6. PERFORMING ORG. REPORT NUMBER
7. AUTHOR(s): PFISTER, RUSSELL J.	8. CONTRACT OR GRANT NUMBER(s)
9. PERFORMING ORGANIZATION NAME AND ADDRESS: Massachusetts Institute of Technology, Cambridge, MA	10. PROGRAM ELEMENT, PROJECT, TASK AREA & WORK UNIT NUMBERS
11. CONTROLLING OFFICE NAME AND ADDRESS: CODE 031, NAVAL POSTGRADUATE SCHOOL, MONTEREY, CALIFORNIA 93940	12. REPORT DATE: May 1979
	13. NUMBER OF PAGES: 113
14. MONITORING AGENCY NAME & ADDRESS(if different from Controlling Office)	15. SECURITY CLASS. (of this report): UNCLASS
	15a. DECLASSIFICATION/DOWNGRADING SCHEDULE

LEVEL II

16. DISTRIBUTION STATEMENT (of this Report)

APPROVED FOR PUBLIC RELEASE; DISTRIBUTION UNLIMITED

17. DISTRIBUTION STATEMENT (of the abstract entered in Block 20, if different from Report)

DTIC ELECTE FEB 12 1982

18. SUPPLEMENTARY NOTES

19. KEY WORDS (Continue on reverse side if necessary and identify by block number)

Mechanical Engineering
Lead-Acid Battery
Shepherd's Equation
Peukert's Equation

20. ABSTRACT (Continue on reverse side if necessary and identify by block number)

SEE REVERSE

82

DD FORM 1 JAN 73 1473 (Page 1) EDITION OF 1 NOV 65 IS OBSOLETE S/N 0102-014-6601

UNCLASS

SECURITY CLASSIFICATION OF THIS PAGE (When Data Entered)

AD A110892

DTIC FILE COPY

ABSTRACT

In order to establish a model which would more accurately predict discharge characteristics of a cell at any arbitrary current, and which would better fit the family of discharge curves, testing was done based on the Shepherd equation using a transparent lead-acid battery.

A set of discharge curves at .6, 1.5, 3.6, and 5.4A, preceded by a 3.6A preconditioning discharge to remove the "memory effect," was obtained. The battery was cycled continuously through deep discharges in an attempt to determine secular changes during the life of the battery.

Several modifications to the Shepherd equation were proposed in order to obtain a better fit to discharge data. These included modeling the capacity as a function of current as $Q=CI^{(1-n)}$, Peukert's equation; modeling the ohmic polarization as a linear function of accumulated charge; and modeling the diffusion polarization as a function of accumulated charge alone and not current.

Conclusions were drawn on the suitability of Shepherd's equation. The inclusion of the changed ohmic polarization term gave a good fit for individual curves which also suggested the change in the diffusion polarization term. Since a small current density approximation was used in Shepherd's equation, developing a model based on the original terms was recommended. Also recommended were the modification of a model to predict characteristics during a cycle with various discharge currents and further life cycle testing to determine the secular changes in the battery.

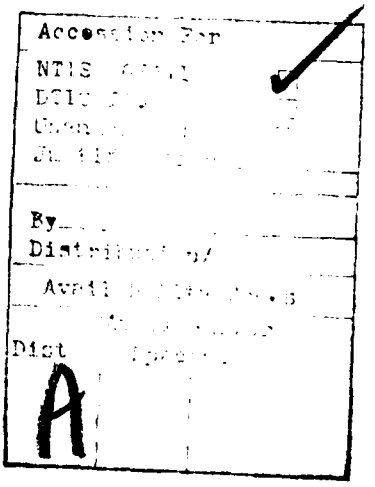

1

ELECTROCHEMICAL STATE MODELS OF LEAD-ACID BATTERIES

by

LIEUTENANT RUSSELL JAMES PFISTER, U.S. NAVY

B.S.E.E., PURDUE UNIVERSITY

1972

SUBMITTED IN PARTIAL FULFILLMENT

OF THE REQUIREMENTS FOR THE

DEGREES OF

OCEAN ENGINEER

and

MASTER OF SCIENCE

IN MECHANICAL ENGINEERING

at the

MASSACHUSETTS INSTITUTE OF TECHNOLOGY

May, 1979

Signature of Author..Russell James Pfister.....
Department of Ocean Engineering, 18 May 1979

Approved by.....
Departmental Reader

Certified by.....
Thesis Supervisor

Accepted by.....
Chairman, Departmental Committee on Graduate Students

ELECTROCHEMICAL STATE MODELS OF LEAD-ACID BATTERIES

by

LIEUTENANT RUSSELL JAMES PFISTER, U.S. NAVY

Submitted to the Department of Ocean Engineering
On 18 May 1979 in partial fulfillment of the requirements
for the Degrees of Ocean Engineer and
Master of Science in
Mechanical Engineering

ABSTRACT

In order to establish a model which would more accurately predict discharge characteristics of a cell at any arbitrary current, and which would better fit the family of discharge curves, testing was done based on the Shepherd equation using a transparent lead-acid battery.

A set of discharge curves at .6, 1.5, 3.6, and 5.4A, preceded by a 3.6A preconditioning discharge to remove the "memory effect," was obtained. The battery was cycled continuously through deep discharges in an attempt to determine secular changes during the life of the battery.

Several modifications to the Shepherd equation were proposed in order to obtain a better fit to discharge data. These included modeling the capacity as a function of current as $Q=CI^{(1-n)}$, Peukert's equation; modeling the ohmic polarization as a linear function of accumulated charge; and modeling the diffusion polarization as a function of accumulated charge alone and not current.

Conclusions were drawn on the suitability of Shepherd's equation. The inclusion of the changed ohmic polarization term gave a good fit for individual curves which also suggested the change in the diffusion polarization term. Since a small current density approximation was used in Shepherd's equation, developing a model based on the original terms was recommended. Also recommended were the modification of a model to predict characteristics during a cycle with various discharge currents and further life cycle testing to determine the secular changes in the battery.

Thesis Supervisor: Professor Henry M. Paynter

Title: Professor of Mechanical Engineering

Acknowledgments

The author would like to express his deep appreciation to Professor Henry M. Paynter of the Massachusetts Institute of Technology for his guidance during his supervision of this thesis and for the example he has set for a quest for new knowledge. He also provided many enjoyable and enlightening hours in lecture, for which the author is very grateful.

The author would also like to thank Captain John Sweeney of the Ocean Engineering Department of M.I.T. for his assistance in providing departmental approval.

Many others were most helpful; among them, Ted Fischer in the Engineering Project Room and Dr. Michael Rosen in the Engineering Rehabilitation Center at M.I.T.

The encouragement of the author's parents, Mr. and Mrs. Medford W. Pfister of Adrian, Michigan, was greatly appreciated.

The author owes a debt of gratitude to his wife, Sheila, for her production of the final copy and continuing support during the entire thesis work. Her "project oriented" manner of approaching tasks was most helpful in the completion of this effort.

TABLE OF CONTENTS

LIST OF FIGURES

LIST OF TABLES

LIST OF SYMBOLS

ΔG	Change in Gibbs free energy	kcal/mole
E_0	Electrochemical potential	volts
	open circuit cell potential	volts
i	current	amps (A)
	current density	amps/cm^2
q	accumulated charge	ampere hours (Ah)
Q	cell capacity	(Ah)
K	mean polarization resistance	ohms Ω
R_0	Internal cell resistance	ohms Ω
t	time	
N	Internal cell resistance	ohms Ω
E	cell potential	volts
V_a	activation polarization	volts
V_d	diffusion (concentration) polarization	volts
V_0	ohmic polarization	volts
E_{rev}	open circuit cell voltage	volts
η_t	charge transfer overvoltage	volts
η_c	concentration overvoltage	volts
I	current	amps
R	resistance	ohms Ω
A_A	surface area of anode	
A_C	surface area of cathode	

LIST OF SYMBOLS (Cont'd)

R	the gas constant	
T	temperature	
z	number of electrons	
F	capacity	Faraday
i_ϑ	apparent exchange current density	amps/cm^2
i_ℓ	diffusion limiting current	amps/cm^2
ϑ	degree of electrode coverage	
	temperature	$^\circ$C
C	constant in Peukert's equation	
n	exponent in Peukert's equation	
E_s	open circuit cell voltage	volt
R_a	linear ohmic resistance	Ω/Ah
R_b	constant ohmic resistance	Ω

CHAPTER 1

INTRODUCTION

1.1 BACKGROUND

Predicting the transient and long-term characteristics of a cell under arbitrary charging and discharging histories is a problem confronting a system designer which could be overcome if there were an electrochemical model of the lead-acid cell. With this model, it would theoretically become possible to determine the optimum scheme for getting energy into and out of a battery.

To what degree is the efficiency of a battery affected by different types of discharge? Should the designer select a pulse-type discharge over a steady discharge? What effect does this have on the system as a whole? To what degree does the age of the battery affect the efficiency? Low current or high? What exactly is the effect of temperature and current on the charging and discharging history of the arbitrary battery? Will current models handle the problem of the age of the battery? Does the model provide a fit merely to a single discharge curve or for the family of curves? Does it account for the condition of the battery? What effect has gassing on the capacity for full charge or discharge? Questions such as these pose a great problem for the designer of a model.

Naturally, there are numerous other criteria which might

affect the optimum charge/discharge history of a battery, so it becomes very important to select a battery type to test which possesses characteristics which are relatively similar to other cells.

The lead-acid cell was chosen for this investigation for several reasons. Lead-acid batteries are the most widely used batteries in the world, and for that reason, they represent the greatest commercial interest. Portable lead-acid batteries have automotive use, use in motorcycles, railroads, all types of military vehicles on the land, sea, and air, and additional uses not related to vehicles.

Additionally, there is a wealth of specific information concerning lead-acid batteries in literature. Volume after volume has been written exploring the numerous characteristics of this type of battery in great detail. Chapters upon chapters have been written about the history, electrochemistry, applications and performance characteristics of lead-acid batteries. Detailed studies have been done on performance and structural aspects, as well as on self-discharge effects.

Because the author chose as the aim of his thesis, the establishment of an electrochemical model of the cell, based on Shepherd's equation (1965), it was necessary to chose a battery type for the experimentation which was rechargable, lightweight, and portable, in addition to having similar characteristics of other types of cells. The lead-acid

battery, in addition to being rechargable, is available in a clear plastic case, thus affording the investigator a visual means to determine some battery conditions which are not readily available empirically in a battery with an opaque case.

Also, it was felt that the characteristics of some of the other types of cells are similar to those of the lead-acid cell and that a model for the one may be applicable to the others.

1.2 HISTORY OF LEAD-ACID BATTERIES

The original incentive toward the development of an electrochemical source of current was the "galvanic cell" which was based on Galvani's "frog leg" experiment, circa 1789.

Volta, after 1792, developed several useful current sources, such as the Volta pile. He also formulated the first electrochemical theory on the subject.

Ritter developed a cell in about 1803, Ritter's pile, which, when disconnected from an external source of current, would yield a current in the opposite direction. This was the basis for the secondary cell or storage battery.

In 1860, Planté demonstrated his cell in which two lead sheets separated by rubber were rolled into a spiral and placed in a 10% sulfuric acid solution. When charged, the amount of energy depended upon the amount of lead oxide formed.

By 1880, W.V. Siemens had invented the dynamo, which was then installed in central power stations. Batteries were used for load leveling purposes, being charged with energy produced at night.

Around 1881, Faure coated the lead foil with lead oxide for the purpose of accelerating Planté's forming process. He used various lead current collector grids.

1883 brought us the Planté plate which was actually designed by Tudor. In this design, he pasted lead oxide onto cast ribbed pure lead plates. Grid plates, plates cast from antimonial alloys were also developed at about the same time.

From 1890 to 1920, wood was used to separate the plates and then rubber. Around 1927, porous ebonite and microporous rubber was used as separators.

Around 1965, batteries were designed to be relatively maintenance-free for use in portable items, and, with the advent of plastic battery cases and lightweight construction, automation and mass-production became feasible.

The 1970s gave us new applications of the lead-acid battery, with increasing interest in Traction batteries coming to the forefront. Water-activated and maintenance-free automobile batteries were designed. Kordesch, (1977)

These historical developments, some important, some merely historically interesting, represent the basis for the lead-acid battery as it is known today.

1.3 THE NEED FOR A MODEL

A system designer needs an accurate electrochemical battery model in order to produce a design which makes optimum use of these batteries. With the use of computer-aided design, a functional description of various battery characteristics would greatly simplify the present cumbersome task of establishing an algorithm for interpolation of battery characteristics from its family of discharge curves. An algorithm for predicting the response to an arbitrary (non-constant current) discharge or charge would be, at the very least, extremely difficult, if not prone to significant inaccuracies.

Several empirical models have been developed in the past to show the dependence of capacity on discharge current I and discharge time t {Schröder (1394), Liebenow (1897), Peukert (1897), Rabl (1936), Davytan (1946), and Shepherd (1965)}. Shepherd's (1965) model (discussed in detail in Chapter II) gives a relationship between cell voltage on discharge as a function of current density and time based on the theoretical laws of electrochemistry. Shepherd's equation (1965) serves as the basis for this investigation into establishing a State Model.

Very early in this investigation, it was found that the equation provided a satisfactory fit to a single discharge curve (complete discharge at constant current) but a poor fit

for the family of discharge curves. A typical family of discharge curves is shown in figure 1-1. Also, Shepherd did not include any term which would account for secular life changes in the cell.

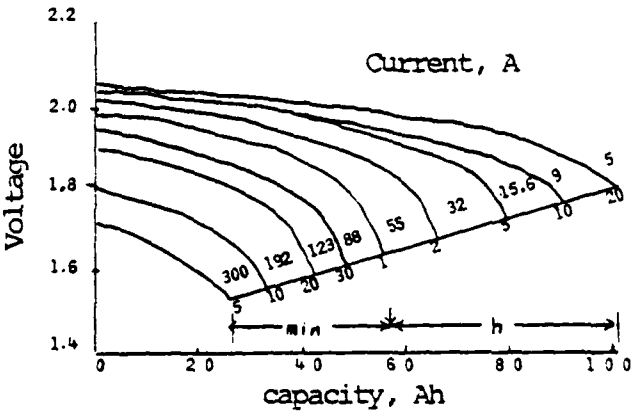

Fig. 1-1. Discharge Curves for a Typical 100-Ah (20-h rate) SLI Lead-Acid Battery.

The emphasis of this thesis was to establish a model which would more accurately predict the discharge characteristics of a cell at any arbitrary current, thereby providing a better fit for the family of discharge curves. Basing his investigation into a State Model on the Shepherd equation

(1965), the author has chosen to call his model the "Modified Shepherd Equation." It was also the desire of the author to experimentally determine the secular life changes of the lead-acid cell and to include a model of these changes in the Modified Shepherd Equation.

The problem of needing an adequate model was made clear to the author while working on a Diesel submarine computer synthesis model at the Naval Ships Engineering Center in Washington, D.C. A great deal of time was invested in establishing a model of the lead-acid cell which would adequately predict the capacity of the cell at arbitrary discharge currents. This was accomplished simply as a curve fit to the capacities determined from the family of discharge curves.

Due to the complexity of the problem, no attempt was made to use the discharge characteristics in that model. If a model such as the one proposed in this thesis had been available, not only would a significant number of man-hours have been saved, but also another degree of flexibility would have been allowed in the synthesis model.

Also, the problem of the design of an electric vehicle is essentially identical in this respect. Moreover, the battery manufacturer, by supplying only a few coefficients for a battery model would be providing the characteristics of his product in a very concise form which would require no interpolation for the user's specific application.

1.4 BATTERY USAGE

Since the earliest "galvanic cell", the lead-acid storage battery has been in demand for numerous purposes. Marine uses alone are diverse.

Marine batteries, which are rugged and durable, have given long service to ships of the Navy and Merchant Marine. These batteries function under extremely adverse conditions and are subject to continual vibration.

These batteries have been used in all types of ships from the largest aircraft carrier to the smallest pleasure craft to power radios, lights, pumps, hoists, and compressors. They are used in torpedoes and to fire guns. They are used in the kitchens of ships to provide power to stoves and refrigerators.

Batteries power alarms and emergency lighting and even pump bilges and hoist anchors. Many are used in ignition circuits of internal-combustion engines of small craft. They provide emergency power for submerged Nuclear submarines and the propulsion for submerged Diesel submarines.

Marine batteries are used for gyrocompass emergency power and for telephones, and emergency generator start-up/ or field flashing.

For many years, scientists and engineers have studied the possibility of converting from gasoline powered motor vehicles to electrically powered motor vehicles, from hybrids to all-electric delivery vans. Much interest was in all-electric

automobiles. It has been found that there are no savings in energy if batteries simply replace the gasoline engine. Electrically powered vehicles would offer a significant pollution advantage over gasoline and Diesel engines. Batteries could be used to provide additional energy requirements in hybrid gasoline/electric vehicles for load leveling purposes or for applications where the possible recovery of energy through regenerative breaking is significant. (Kordesch 1977)

Batteries have been classified according to usage, according to Bode (1977):

1. SLI Batteries (Starting, Lighting and Ignition)

   These batteries are used to start an internal-combustion engine and to provide power to the electrical system when the engine is not running. The largest number of storage batteries are for use in the automobile and are used for this purpose more than for any other.

2. Stationary Batteries

   These generally provide emergency power when the primary source of power is not available. These include such applications as communications systems, electric utilities, computer systems, emergency lighting, and railways to provide peak loads, emergency power or smoothing of ac power.

3. Motive Power (Traction) Batteries

Lead storage batteries provide power for the propulsion of devices such as electric lift trucks, mining equipment, street delivery vehicles, and other types of material handling.

4. Special Purpose Batteries

Some examples of batteries in this category are aircraft, submarine, special military and small sealed batteries for consumer applications. Some of these uses have already been discussed.

1.5 BATTERY LIFE

The life of a battery can be defined as the period of time during which it has the ability to perform within certain specified limits. In other words, the end of life occurs when the battery can no longer perform within these limits. These limits actually depend upon the application and the requirements of the system they serve. The end of life of an automobile battery occurs when it no longer is able to provide sufficient cranking power to start the engine. For a battery powered vehicle, it may be when the vehicle will no longer travel a certain number of miles at a specified speed; in traction batteries, the decrease of capacity below a certain value may be the criterion on which the end of life decision is based. Generally, however, systems are designed to meet all specified requirements as long as the battery is able to deliver 80% or more of its new capacity.

Bode (1977) states that the end of battery life is best evaluated in the laboratory using fixed standards and specified test conditions. The ideal requirement is that the life test correspond to the load conditions of the battery in the field, however, as in the case of automobile batteries, ideal testing in the laboratory is impossible because it is impossible to duplicate such diverse conditions as automobile type, driving methods, maintenance and environment. Figure 1-2 is a plot of the change in capacity during the

lifetime of a lead-acid battery. Very little information is available which provides details on the change of characteristics of a cell during its lifetime. It is therefore proposed that this data be obtained by experimental means.

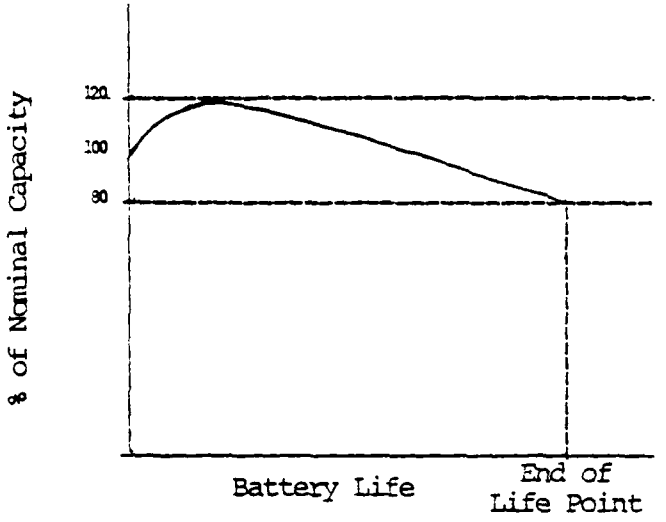

Figure 1-2. Typical Cell Capacity During the Lifetime of a Lead-Acid Battery. KORDESCH (1977)

The discharge capacity of a battery has been found to be somewhat dependent upon the rate of previous discharges. Bode (1977) calls this the "memory effect." Vinal (1955) states that "the capacity is lower if the discharge has been preceded by a discharge at a higher rate, and it is higher if preceded by a discharge at a lower rate." Therefore, any experimental procedures should take the "memory effect" into consideration.

1.6 REASONS FOR DECREASE IN LIFE EXPECTANCY OR FAILURE

According to Vinal (1955), storage batteries large and small and in widely diverse services are subject to conditions that may lead to excellent service or through accident or abuse to something less than satisfactory. Under his heading "Sources of Trouble," he writes about faulty conditions which if detected could be corrected. Detection and correction of faulty conditions might prolong the satisfactory battery life into years.

He also states that as a result of studies done in 1947 on thousands of worn out batteries which had been used in normal service, the reasons they wear out became well known. In comprehensive data relating primarily to automobile batteries, grid corrosion of the positive plates accounted for 42% of the total failures. Naturally, with the use of new alloys, batteries developed since that time should have less positive plate corrosion.

Bode (1977) indicates that destruction of the positive grids occur when lead sulfate forms a heavy layer on the grid to protect it from being dissolved anodically. One rarely encounters corrosion of the negative grid. Hydrogen corrosion occurs in the presence of organic substances and at higher operating temperatures. The result of corrosion is loss of conductivity and grid breakage.

Vinal (1955) indicated that 7 to 10% had less than total life span due to shedding of positive active material, cracked partitions and leaking cases accounted for nearly one-third, and buckled plates and short-circuited separators produced failure in 10 to 12% of the batteries. About 10% of the failures were caused by negative plate failure. Sulfation which causes buckled plates and negative failures, was a cause of battery failure in less than 20% of the batteries.

Overcharging loosens active material, corrodes positive grids, causes excessive gassing and produces sludging of a fine brown sediment. It may cause raised temperatures contributing to battery destruction with damage to plates and separators, buckling of plates and needless loss of water.

Bode (1977) states that in sulfation, "hard" lead sulfate forms if chargeable lead sulfate undergoes long or high temperature aging process, (recrystallization). Sulfation produces loss of capacity and is caused by long standing in a discharge condition, too high acid concentration, increased self-discharge, continuous operation between 45° and 50°C, and prolonged undercharging.

He also indicates that sludging of the positive mass occurs most at the end of a charge and at the beginning of a discharge. Heavy gassing facilitates sludging. There is a greater amount of sludging in discharges with large current density. The type of discharge influences sludging. If acid

concentration is drastically reduced, temperature increases or current density is diminished, there is less sludging and the battery life is increased.

Vinal (1955) concludes that occasional overcharging is beneficial, but habitual overcharging decreases useful battery life.

He indicates that undercharging gradually runs down cells producing diminishing values of specific gravity. Plates become lighter in color and a sludge, a fine white powder which is predominantly lead sulfate, is produced. One or more cells could become exhausted. He concludes that the remedy is to charge until all cells are in normal condition. This is referred to as an equalizing charge. Undercharging is the most common cause of buckling of plates because lead sulfate occupies more space than the original material producing excessive strain on the plates.

Failure of the charging system and of the battery ultimately is blamed on the battery. When an automobile reaches speeds greater than or equal to 12 to 15 mph the battery begins to charge. If the generator doesn't come on at the proper speed the battery won't receive its required amount of charge. Also, the system must regulate itself properly so that the battery will not receive massive amounts of current when the automobile reaches highway speeds. Conditions in the charging

system which drain the battery and cause it to remain discharged are grounded circuitry and partial grounds. (Vinal, 1955)

Other possible causes of shortened battery life include corroded terminals, short circuits, separator failures, worn-out plates, electrolyte below the tops of the plates, freezing, when the battery is in a discharge condition, impurities in the solution, spalling of the active material, growth of positive plates, shrinkage of negative plates, leading, and battery explosions. The interested reader is directed to the classic text of Vinal (1955) and the excellent texts of Bode (1977) and Kordesch (1977).

CHAPTER 2

THEORETICAL ANALYSIS

2.1 ELECTROCHEMISTRY OF THE LEAD-ACID BATTERY

The theory of operation of the lead-acid battery is based on the "double sulfate theory" proposed by Gladstone and Tribe, (1881-1883).

$$PbO_2 + Pb + 2H_2SO_4 \underset{\text{charge}}{\overset{\text{discharge}}{\rightleftharpoons}} 2PbSO_4 + 2H_2O \qquad (2.1)$$

The principle was so named because the discharge product of both the lead anode electrochemical oxidation reaction and the lead dioxide cathode electrochemical reduction reaction is lead sulfate.

This early equation reveals the stoichiometric relationship of reactants and products, as well as the role played by the sulfuric acid.

A more complete representation of the actual electrochemical reactions is:

$$\text{ANODE:} \quad Pb + HSO_4^- \underset{\text{charge}}{\overset{\text{discharge}}{\rightleftharpoons}} PbSO_4 + H^+ + e^- \qquad (2.2)$$

$$\text{CATHODE:} \quad PbO_2 + 3H^+ + HSO_4^- + 2e^- \rightleftharpoons PbSO_4 + 2H_2O \qquad (2.3)$$

$$\text{OVERALL:} \quad Pb + PbO_2 + 2H^+ + 2HSO_4^- \rightleftharpoons 2PbSO_4 + 2H_2O \qquad (2.4)$$

The electrolytic dissociation of sulfuric acid into H^+ and HSO_4^- is closer to the true picture in the cell. The dissociation into $2H^+$ and SO_4^{-2} occurs in solutions much more dilute than those found in a lead-acid cell.

During overcharge, the electrolysis of water occurs, yielding hydrogen and exygen.

Based on the free-energy change of

$$\Delta G = -13.95 \text{ kcal/mole}$$

for the anodic reaction

$$(E_0 = 0.303 \text{ V versus } H_2/H^+)$$

and

$$\Delta G = -74.99 \text{ kcal/mole}$$

for the cathodic reaction

$$(E_0 = -1.627 \text{ V versus } H_2/H^+),$$

the overall reaction values are:

ΔG = -88.94 kcal/mole

(E_0 = 1.93 V)

specific energy = 161 Wh/kg

specific capacity = 83.5 Ah/kg

Bode (1977).

In practice, significantly lower specific energies are exhibited, but the theoretical values provide an upper limit to possible future developments. For a complete discussion of electro-chemical theory, the reader is directed to the excellent text by Bode (1977), and the classic text in the area by Vinal (1955).

2.2 THE SHEPHERD EQUATION

Shepherd (1965) has proposed a static model for cell discharge characteristics which uses simple analytical expressions of chemicophysical origin and describes the cell potential E as follows:

$$E(q,i) = E_0 - V_a(q) - V_0(i) - V_d(i,q) \qquad (2.5)$$

where E_0= open circuit cell potential

$V_a(q) = A \exp\left(-\frac{Bq}{Q}\right)$ = activation polarization

$V_0(i) = R_0 i$ = ohmic polarization

$V_d(i,q) = K\left(\frac{Q}{Q-q}\right) i$ = diffusion (concentration) polarization

i = the discharge current

q = it = the accumulated charge

Q = the cell capacity

K = the mean polarization resistance

R_0 = the internal cell resistance

Shepherd used "it" in place of "q" in his equation and R_0 corresponds to his N. The activation polarization term is the single term which does not have any particular theoretical basis. Its inclusion accounts for the rapid drop in potential at the beginning of discharge. Figure 2-1 shows an exagerated view of this phenomenon. The time

duration of this initial drop was found to be in order of seconds. Consequently, the description of cell discharge should not be significantly affected by simply ignoring the term; this was the approach used by Shepherd, also.

Another phenomenon shown in fig. 2-1, not treated by Shepherd, is known as the "voltage dip" or "coup de fouet" where initially the voltage drops below the "steady state" value and then rises to this level within a few minutes.

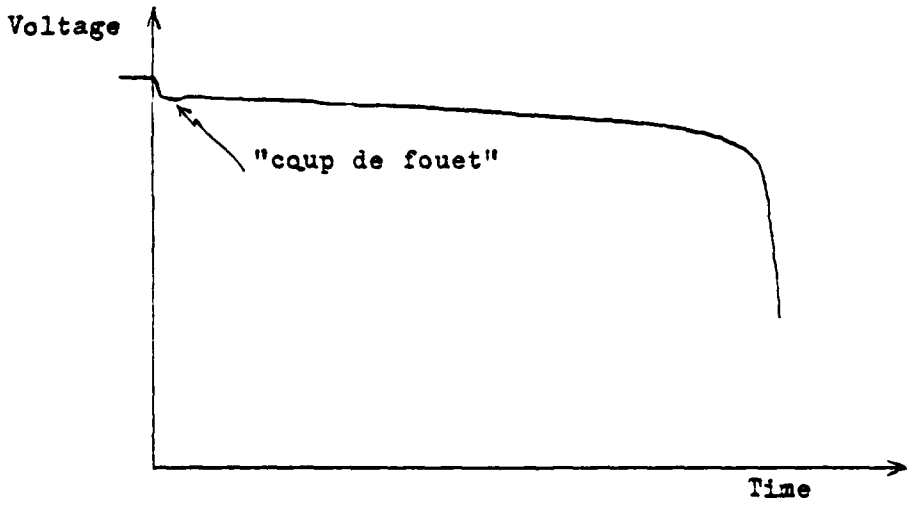

Figure 2-1. Cell Voltage versus Time for a Constant Current Discharge

The ohmic polarization term accounts for the ohmic resistance through both the metal and the solution. This has been modeled as a constant, however, it is felt that this assumption may be erroneous.

The specific electrical resistance of lead oxide is on the order of 10^{-6} Ω/m and metallic lead, on the order of 10^{-7} Ω/m. The electrolyte has a range of specific resistance of about 125 Ω/m when nearly fully charged to about 170 Ω/m when discharged. The product of the two reactions, lead sulfate, is highly resistive, specific resistance on the order of 10^{10} Ω/m. Based on these values, it would be expected that the ohmic resistance increase as the reaction proceeds and becomes fairly significant as it approaches completion.

The diffusion (concentration) polarization term appears to have been made up from a combination of what Bode (1977) calls the charge transfer overvoltage, η_t, and the concentration overvoltage, η_c. Following Bode's development, the terminal voltage of the cell is

$$E = E_{rev} + (\eta_t + \eta_c)_A - (\eta_t + \eta_c)_C - IR \qquad (2.6)$$

E_{rev} is the open circuit voltage and IR includes the resistances of the electrolyte and separator. The subscripts A and C refer to the anode and cathode overvoltages, respectively. All of the overvoltages decrease the cell voltage on discharge, and overvoltages of the electrodes are related to the current densities, i. Assuming that the electrodes have equal surface area $A_A = A_C = A$, then for both electrodes the

following expressions apply:

$$\eta_t = \frac{2.3\ RT}{zF} \log i_0\ (1 - \Theta\ ) - b \log i \qquad (2.7)$$

and

$$\eta_c = \frac{2.3\ RT}{zF} \log\ (1 - \frac{i}{i_\ell}\ ) \ . \qquad (2.8)$$

For small current densities, these become

$$\eta_t = \frac{RT}{zFi_0(1 - \Theta)} \qquad (2.9)$$

and

$$\eta_c = \frac{RT}{zF}\ \frac{i}{i_\ell} \qquad (2.10)$$

For this case, one of the terms in (2.6) may be neglected if they differ by an order of magnitude. The terms in the equations above are:

i_0 = the apparent exchange density

z = the number of electrons transferred in the determining step

F = the Faraday (measure of capacity)

R = the gas constant

T = the temperature

i_ℓ = the diffusion limiting current

and

Θ = the degree of coverage. (only the uncovered portion $(1-\Theta)$ of the electrode can react)

Replacing the constant terms in η_t by a single constant k yields

$$\eta_t = \frac{K}{(1 - \theta)} \tag{2.11}$$

If the uncovered portion of the electrode is related to the cell capacity Q and accumulated charge q where $q \leq Q$ with $q \to Q$ at complete discharge, equation (2.11) becomes

$$\eta_t = \frac{K}{(1-\theta)} = K \frac{Q}{(Q-q)} . \tag{2.12}$$

This term is similar to Shepherd's diffusion polarization but with the striking difference that it is not a function of current. If one were to fit Shepherd's equation to a single discharge curve, this difference would not be apparent because the product of K and i in equation (2.5) would be equal to K in equation (2.12).

Prior to the discovery of the above relationship, the author, while attempting to make a fit for a family of discharge curves to Shepherd's equation, produced fits of each curve individually. In the process of analyzing these results a rather surprising discovery was made in that the product of K and i was nearly constant.

Another item in Shepherd's equation which should be addressed, is the cell capacity, Q. The value for Q should be close to the capacity of the cell at the particular discharge

current. In fact, it needs to be slightly larger than the actual capacity to avoid predicting infinite overvoltages, i.e. $Q > q$ for all values of q at the particular discharge current.

The most widely used model for all capacity is Peukert's (1897) equation,

$$I^n t = C \ . \tag{2.13}$$

In this equation n and C are constants which can be determined by using the discharge rate and time for complete discharge at two different currents. Since the cell capacity in terms of Q is the desired quantity, the substitution of $t = Q/I$ gives

$$I^{(n-1)}Q = C \quad \text{or} \quad Q = CI^{(1-n)} \tag{2.14}$$

The values of n and C can be calculated as follows:

$$Q_1 = C\ I_1^{(1-n)}$$

$$Q_2 = C\ I_2^{(1-n)}$$

$$(n-1)\log I_1 = \log C - \log Q_1$$

$$(n-1)\log I_2 = \log C - \log Q_2$$

$$n = \frac{\log Q_2 - \log Q_1}{\log I_1 - \log I_2} + 1$$

The value for n is in the range of from 1 to 2. For diminishingly small current densities, n approaches 1 and for high current densities, n approaches 2. Typically, the value of n falls within about 1.3 to 1.4 This equation is not based on any particular physical laws, but serves as a good empirical fit to discharge capacities.

Baikie, Gillibrand, and Peters (1972) expanded on this relationship to include temperature effects in the range of $-18^{\circ}C$ to $+16^{\circ}C$; for current densities between 21 and $165 mA/cm^2$ it has the form

$$Q = \frac{K_0(1 + \alpha\theta)}{I^{(n-1)}} \qquad (2.15)$$

Where Q is the effective plate capacity, and θ is the temperature in $^{\circ}C$. The values they established were

$$n = 1.4 \text{ for both plates}$$

$$K = 0.32 \text{ and } 0.24 \text{ min},$$

and

$$\alpha = 0.021 \text{ and } 0.015 \text{ min}/^{\circ}C$$

for the negative and positive plates, respectively.

Even if these equations provide a perfect correlation to the capacity of a cell, they do so only at one instant and do not predict changes which occur throughout the life of the battery. If a state model is to be established for the electrochemical cell, then these effects must also be included.

2.3 METHOD OF DETERMINING COEFFICIENTS FOR THE MODEL

An iterative approach using a digital computer was used to determine the coefficients for the model. This curve fitting method basically used the following steps:

1. Choose initial values
2. Vary each value independently

   Trial Value = Value * $(\text{Factor})^{n}$

   where n = -1,0,1 and 0 Factor 1
3. Choose the set of trial values which gives the smallest difference between the data and model.

Steps 2 and 3 were repeated until no further improvement was required by the user. When the "best" set of values was found, then these trial value were used in the next iteration as the values. When a particular factor failed to make any improvement, the difference between the factor and 1 was reduced by 1/2 and a new iteration was performed.

For runs of the Shepherd equation, initial values were chosen such that:

E_s = open circuit voltage

Q = cell capacity plus a small amount to prevent division by zero

Ki + Ri = E_s - discharge voltage at t = 0.

This method finds a minimum value for the correlation, but the only assurance is that the set of values corresponds to a relative minimum.

CHAPTER 3

EXPERIMENTAL PROCEDURE

3.1 BATTERY CHARACTERISTICS

In order to establish a model which would more accurately predict the discharge characteristics of a cell at any arbitrary current and throughout its life, testing was performed using a lead-acid battery.

The type of battery used was a low capacity motorcycle type battery in a clear case. The low capacity was used so that the equipment could be chosen requiring smaller current carrying capacities. The advantage of the clear case over an opaque case was that the author could more readily observe conditions of the battery, including the amount of gassing during charging, the level of the electrolyte, the changes, if any, in the condition of the plates and the accumulation of any sludge, or fine-grained sediment, in the bottom of the battery case without destroying the battery in order to make these observations.

Table 3-1 lists the battery specifications and overall dimensions. Figure 3-1 shows the internal configuration of a cell. Each cell was configured with anode (-) plates on the ends. As can be seen, in the figure, there are four anode (-) plates and three cathode (+) plates with 6 separators in the spaces between the plates.

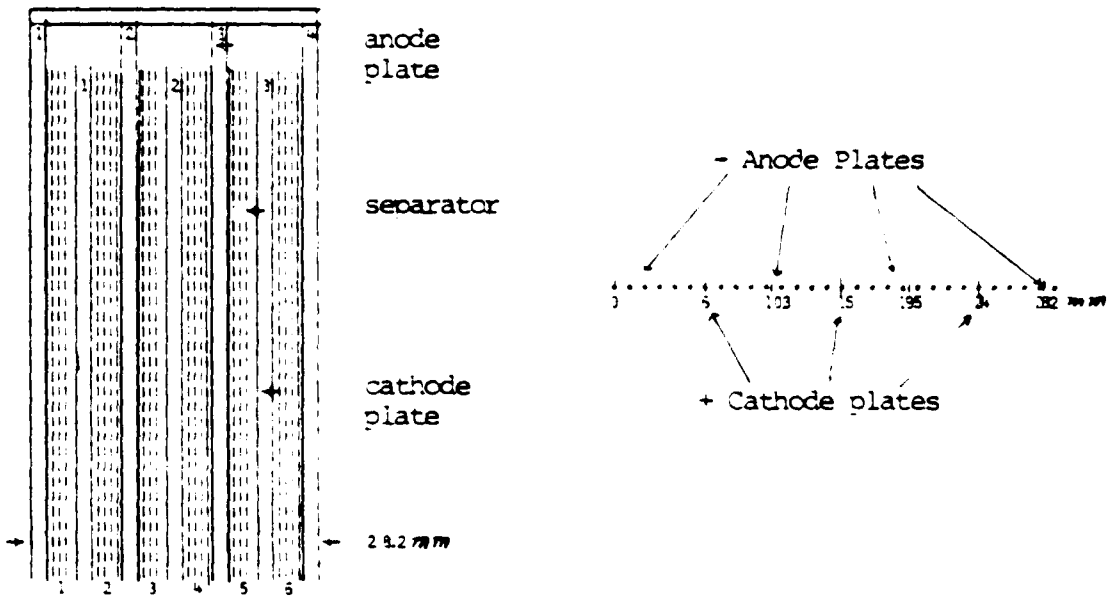

Figure 3-1. Internal Configuration of a Cell.

Manufactured for:	Wisco Division ESB Incorporated 1222 18th Street Racine, WI 53403
Battery Type:	JA-11 6V 3 Cell
JIS Designation:	6N6-3B
Capacity:	6Ah @ 10-h rate
Case:	Clear Plastic Bottom with Black Plastic Top
External Case Dimensions:	L = 10.7cm W = 5.5cm H = 11.0cm

Table 3-1. Battery Specifications and Dimensions.

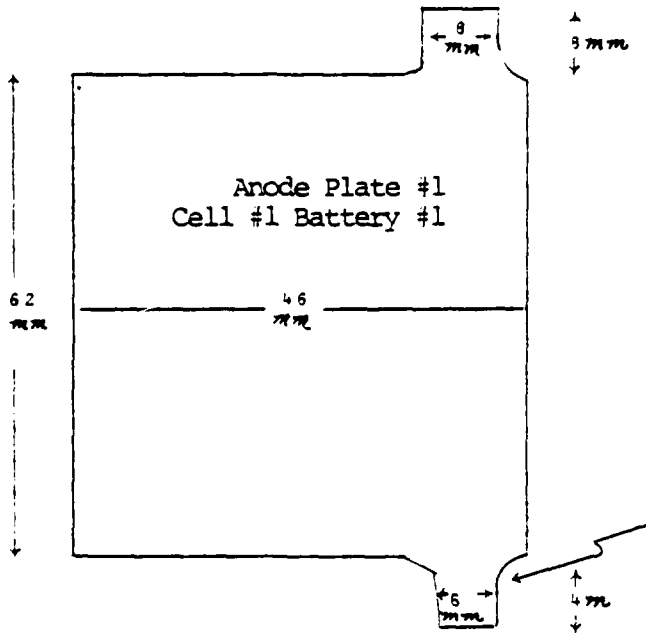

Connector

Note: All plates appear to have the same dimensions.

Area $\overset{\sim}{=}$ 29cm

Note: This tab supports the plate on a rib in the case running the length of the cell.

Figure 3-2. Side View of Anode Plate #1 as Seen from the End of the Battery.

Table 3-2 lists the measurements on cell #1 to determine the thicknesses of the plates and separators. These measurements were made by placing a rule against the side of the case. Some degree of uncertainty in the measurement of the plate thicknesses can be attributed to the method of measurement required.

Figure 3-2 shows the side view of anode plate #1 which is the view seen when looking at the end of the battery. All plates have essentially the same dimensions. The area of the plates is approximately 29cm^2.

COMPONENT	DISTANCE (mm)	THICKNESS (mm)
Anode Plate #1	1.5	1.5
Separator #1	4.0	2.5
Cathode Plate #1	6.2	2.2
Separator #2	9.0	2.8
Anode Plate #2	10.3	1.3
Separator #3	13.0	2.7
Cathode Plate #2	15.0	2.0
Separator #4	17.7	2.7
Anode Plate #3	19.5	1.8
Separator #5	22.0	2.5
Cathode Plate #3	24.0	2.0
Separator #6	26.5	2.5
Anode Plate #4	28.2	1.7

AVERAGE THICKNESS	
Anode	1.575mm
S. Dev.	0.222
Var.	0.0369
Cathode	2.07mm
S. Dev.	0.115
Var.	0.0089
Separators	2.62mm
S. Dev.	0.133
Var.	0.015

Table 3-2. Measurements of the Distances of the Components from Edge of Anode Plate #1 and the Thicknesses of the Anode and Cathode Plates and Separators.

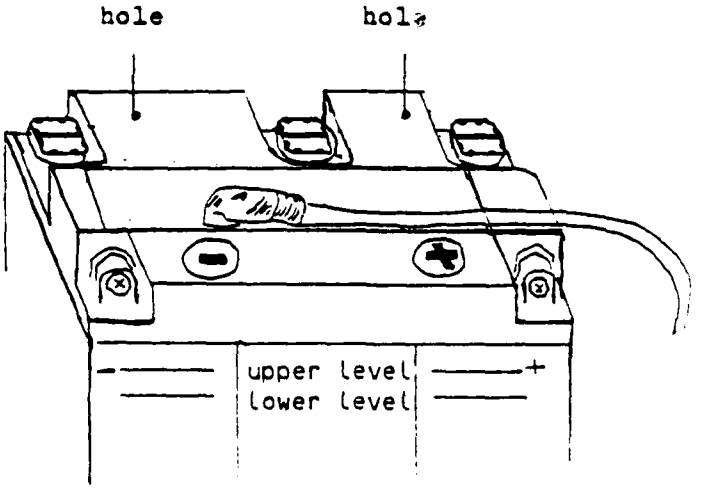

Figure 3-3. Top View of Test Battery

Table 3-3 shows the volume of the materials in a cell, including the deduced volume of electrolyte of 80cc.

Access to the connectors between cells #1 and #2, and cells #3 and #4 was made by drilling into the top of the case. The location of the holes is shown in figure 3-3.

The following observations were made of the battery in its unused condition. The anode plate viewed from the side had a light grey appearance; viewed from the end it was darker grey. Bubbles were seen on the plate and periodically several would rise to the surface. Cathode plates could only be observed from their ends due to the configuration of the cells. They had a dark brown rusty coating on their surfaces. Bubbles were not

INTERNAL VOLUME (per cell):

L = 29mm
W = 51.5mm
Height to upper electrolyte level (marked on case) = 80mm

Volume ≅ 120cc

VOLUME OF ELECTROLYTE:

Vol. of anode (per cell) = 29cm * .1575cm * 4 = 18.3cc
Vol. of cathode (per cell) = 29cm * .207cm * 3 = 18.0cc

Internal volume - plate volume = 120cc - 36cc = 84cc
Assume solid volume of separators = 4cc

VOLUME OF ELECTROLYTE = 80cc/cell

Table 3-3. Volume of Materials within a Cell.

generally observed on these plates.

These observations were made several weeks after the batteryhad first been activated, but before it had been used. When the battery had first been activated, the anode and cathode plates had more nearly the same appearance, which was light grey.

The separators appeared to be made of a "fiber wool" placed on a paper (or felt) backing. The backing was always placed against the anode plates, while the "wool" was against the cathode plates. Small bubbles were entrapped in the fiber.

The cavity below the plates had a very slight amount of rusty-colored, fine-grained sediment.

3.2 EXPERIMENTAL SET-UP

Figure 3-4 is a circuit diagram of the experimental set-up using a double pole-double throw switch. The circuit was configured in this manner so that no disconnecting and reconnecting would be required between charges and discharges and a single ammeter could be used in either mode.

Two different battery charging set-ups were used. One was simply the use of a commercially available 6 Volt Tapering-Type battery charger. The battery charger was manufactured by Mallory, Indianapolis, Indiana (Engineering Projects Lab Number 1167), Model 6SAC10.

Two chart recorders were used. One was a 4 channel chart

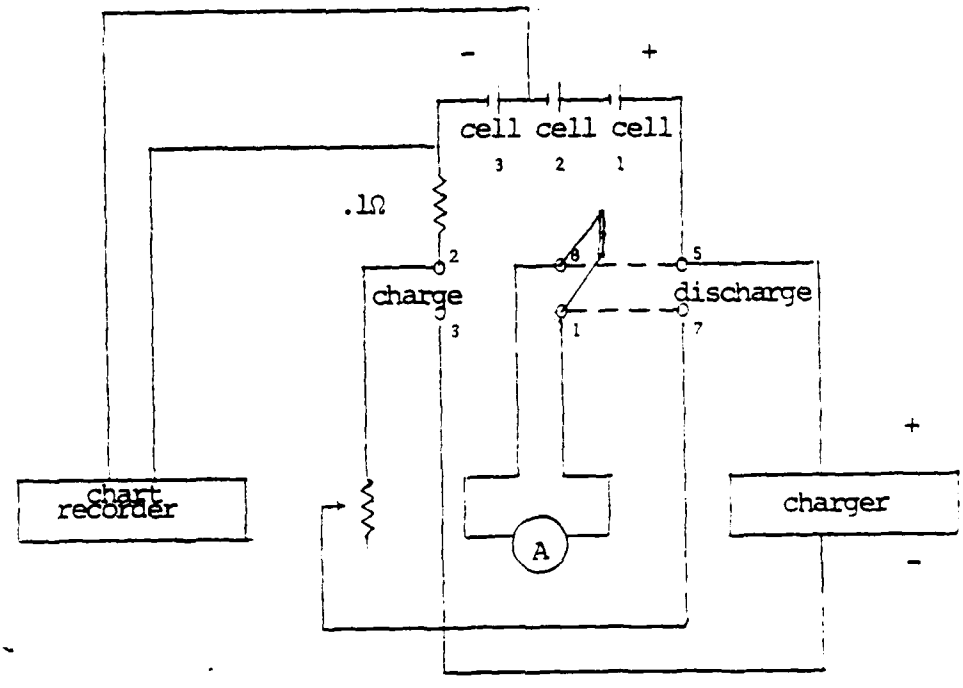

Figure 3-4. Circuit Diagram of the Experimental Set-Up Using a Double Pole-Double Throw Switch.

recorder manufactured by Gould Brush 2400 Model 2007-4404-00 Serial 00473. All four channels were used to record the voltage on each cell and the current simultaneously. This provided the experimenter with a complete picture of the behavior of the battery.

The single channel chart recorder, a Hewlett-Packard Mosley 680 Strip Chart Recorder, Model H01-680, Serial # 712-01825 (Engineering Projects Lab #1175) was used to record the voltage of the cell with the lowest capacity, i.e., the

cell which controlled the end of discharge point. This was cell #3 in battery #2. The single channel chart recorder was used twenty-four hours a day during life cycle testing, primarily because its slowest speed of 1 inch per hour gave a concise record of charge/discharge cycling.

The four channel chart recorder was used when a more complete picture of the charge/discharge cycles was desired. The slowest speed on this chart recorder was 5mm per 100 sec (approximately 7 inches per hour). Continuous running would have produced an unmanageable amount of paper.

The set-up for life cycle testing included a sensing circuit to determine the end of discharge and end of charge and a relay to perform the switching of the battery circuit, as shown in figure 3-4. Figure 3-5 shows the schematic of the sensing and relay-driving circuit. The sensing circuit is a Schmitt Trigger described by Millman and Taub (1965).

It is a bistable circuit, and for a loop gain greater than 1, its input-versus-output displays hysteresis, as shown in figure 3-6.

The relay driving circuit simply consists of a single transistor connected in series with the relay, with the output of the Schmitt Trigger to the base of transistor Q3. The diode connected across the relay was simply for the purpose of providing positive opening of the relay when the driving

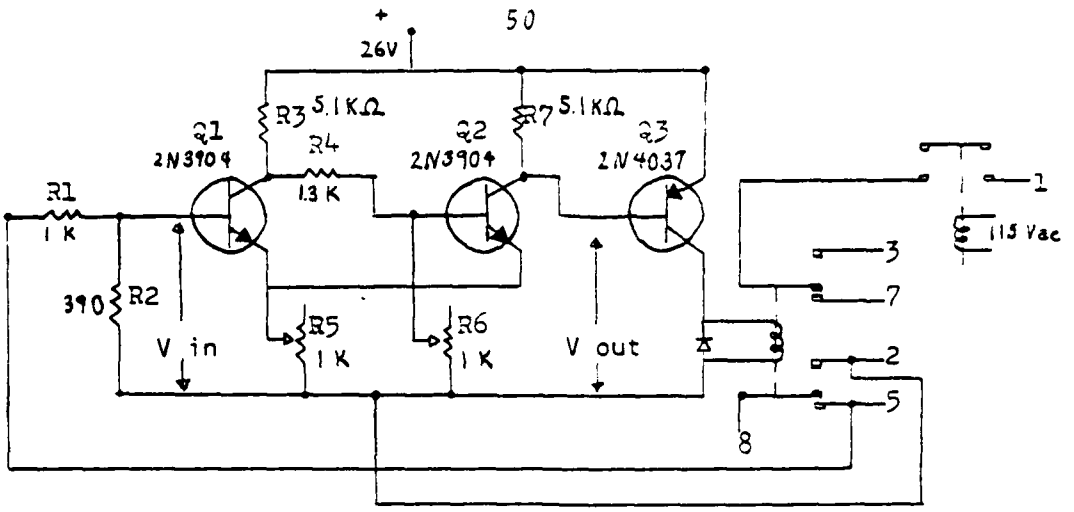

Figure 3-5. Schematic Diagram of the Schmitt Trigger Sensing and Relay-Driving Circuit.

transistor turns off. The other relay shown in the circuit was included as a fail-safe device. It is energized by 115V ac line power. Its terminals are connected in series with the ammeter so that if there is a loss of power, the battery circuit is opened. The terminals of the main relay were wired to the terminals of the double pole-double throw switch through a plug. When it was desired to perform controlled testing of the battery, the sensing and relay circuit was unplugged.

One recommended modification to the circuit is to insert a 3 position switch to the base of the driving transistor Q3. One position would connect the Schmitt Trigger to the tran-

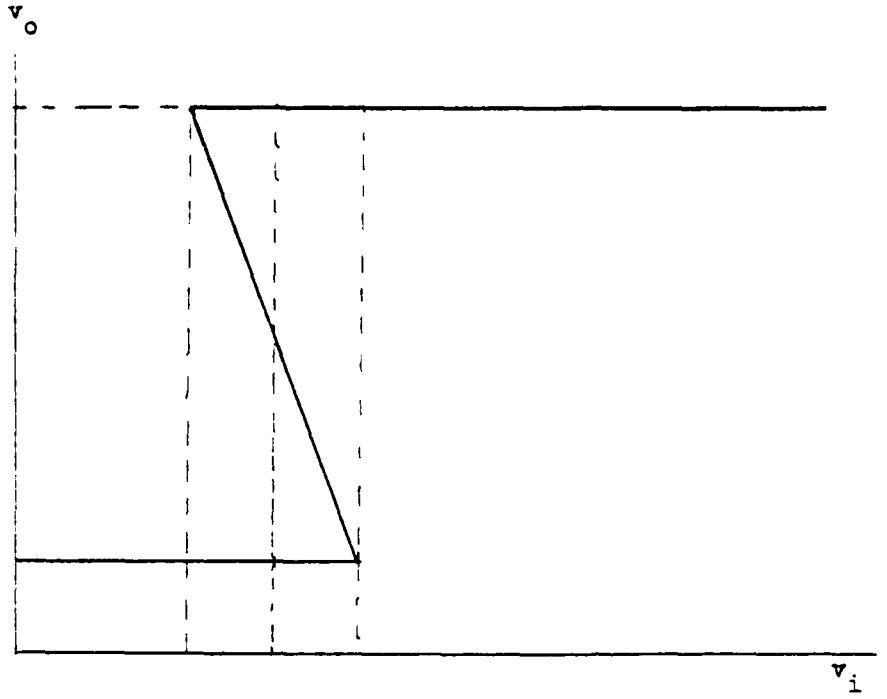

Figure 3-6. Hysteresis of Schmitt Trigger Circuit.

sistor, as shown in figure 3-5. Another would bias Q3 off, placing the battery on discharge, while the third position would turn Q3 on placing the battery on charge. This would facilitate making the controlled charges and discharges. Also, a simple open or closed switch in the fail-safe relay line might be added. With the set-up as shown, it was necessary to unplug the relay's energizing power from the wall receptacle.

The Schmitt Trigger was very sensitive to fluctuations of short time duration. This might be improved by inserting small capacitors from the base of Q1 and Q2 to their emitters.

3.3 TESTING PROCEDURE

There were basically two objectives of the testing. One was to experimentally obtain a family of discharge curves for the verification or modification of the Shepherd (1965) equation. The other was life-cycle testing in order to determine the change in battery characteristics with age.

To obtain a family of discharge curves, constant current discharges were performed at 0.6, 1.5, 3.6, and 5.4A. These values were chosen because it was expected that they would provide a range of values similar to those shown in a plot of typical curves, such as those in figure 1-1. Once two runs have been made at different currents, Peukert's (1897) equation can be used to determine the current required for the discharge times desired.

In an effort to place the battery in identical conditions prior to a discharge in which the data would be used for comparisons, the following procedure was followed. The battery was fully charged, followed by a pre-conditioning discharge at 3.6A. The reason for the pre-conditioning discharge was to remove variations in the "memory effect" (discussed in Section 1.5) caused by previous discharges. The pre-conditioning discharge was followed by a constant current charge of 3.0A. The constant current was maintained by the use

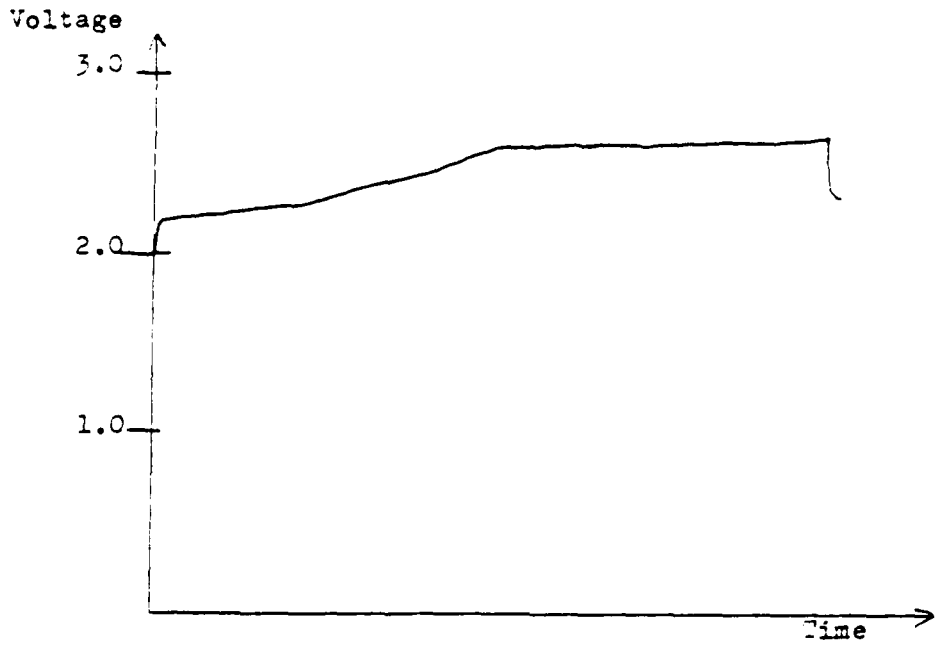

Figure 3-7. Typical Charging Curve at Constant Current of 3.0A.

of a 12 Volt battery connected in series with a variable resistor and was used as a charger.

These values were chosen because they were within the range of currents used during life cycle testing and for convenience. By using this scheme, it was felt that repeatable results could be obtained. The end of charge was determined to occur when the battery was gassing heavily and the cell voltage had remained constant for about 10 to 15 minutes, as shown in figure 3-7.

Prior to discharging the battery, it was left on open

circuit for a period of at least one hour but not generally more than twelve hours. This would allow the electrolyte to become fairly uniformly distributed throughout the cell and also for the temperature to stabilize.

During discharge, the variable resistor which served as the load was adjusted periodically to maintain constant current. The end of discharge occurred when the voltage of a cell dropped off abruptly. Discharge was terminated when this voltage dropped to approximately 1.0V.

Life cycle testing was performed using the Schmitt Trigger circuit and relay with the Mallory battery charger and a constant load resistance of about 1.6Ω. The charging current was in the vicinity of 3.0A, ranging from 3.5 at the start of charge to about 2A at the end. The average discharge current was in the vicinity of 3.5A. The Schmitt Trigger circuit was set to end discharge and commence charging when the battery voltage dropped to about 5V, and to switch on the high end at about 7.5V. The setting at the low end could vary by as much as several tenths of a volt without any particular change in the time of switching, due to the very rapid fall off of voltage at this point. The setting at the high end needed to be much more precise due to the leveling off of voltage at the fully charged point. This proved to be most difficult and introduced variations in the state of charge at the commencement of discharge under life cycle testing.

CHAPTER 4

RESULTS AND DISCUSSION

4.1 MODIFICATIONS TO THE SHEPHERD EQUATION

The numeric data corresponding to figures 4-1 through 4-36 in this section is found in appendix A. Figure 4-1 shows the family of discharge curves obtained following the methods outlined in Section 3.3. Figure 4-2 shows the same curves after manual smoothing. One of the primary effects of this smoothing was the removal of the initial rapid drop of voltage, which Shepherd accounted for in his activation polarization term, and the "coup de fouet." Since the initial drop was completed within seconds of starting the discharge, and the "voltage dip" had disappeared within about two minutes, ignoring these phenomena should have little effect on the applicability of a model.

The first step toward the establishment of a model was an attempt to fit the discharge data to Shepherd's equation:

$$E = E_s - K \frac{Q}{Q - q} i - R_0 i$$

The values found by a least squares fit were:

$$E_s = 2.295$$

$$K = 0.08086$$

$$Q = 6.844$$

$$R_0 = 0.00092$$

with a correlation $\Sigma (E - E_{exp})^2$ for all curves = 3.5008.

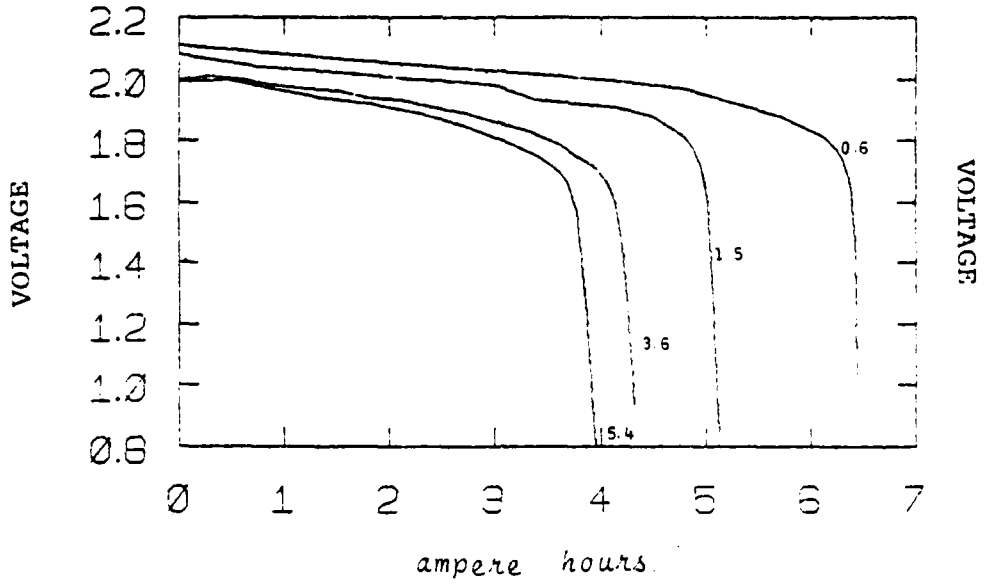

Figure 4-1. Family of Experimentally obtained Discharge Curves.

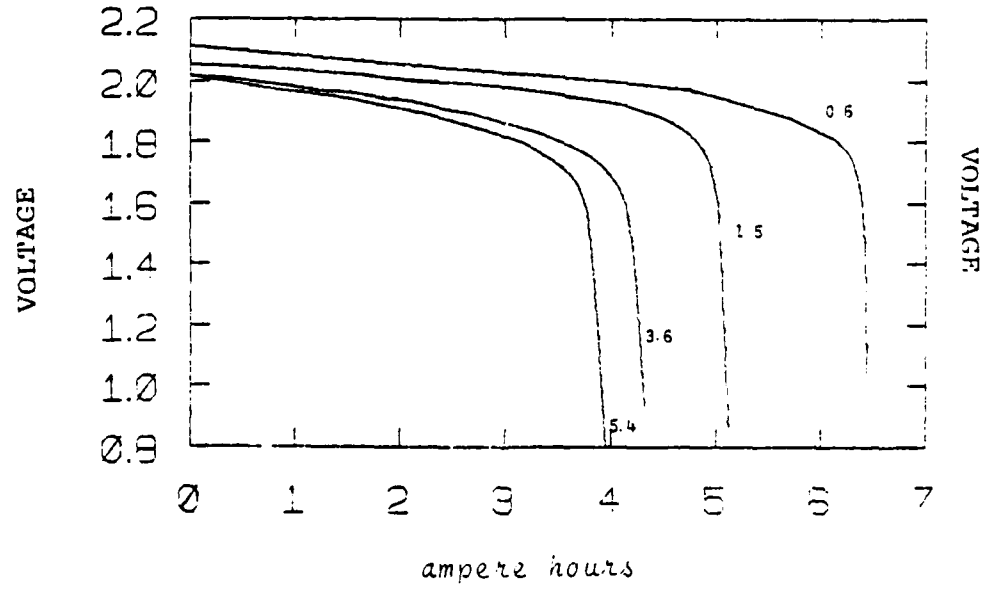

Figure 4-2. Smoothed Family of Discharge Curves.

Figure 4-3 shows the resulting family of discharge curves. Comparisons of each individual discharge curve and its corresponding modeled discharge curve are shown in figures 4-4 through 4-7.

These results illustrate the need for some modification. The rapid drop-off of voltage at the end of discharge was only predicted for the .6 amp discharge. This was the expected result, considering the denominator of the concentration polarization term.

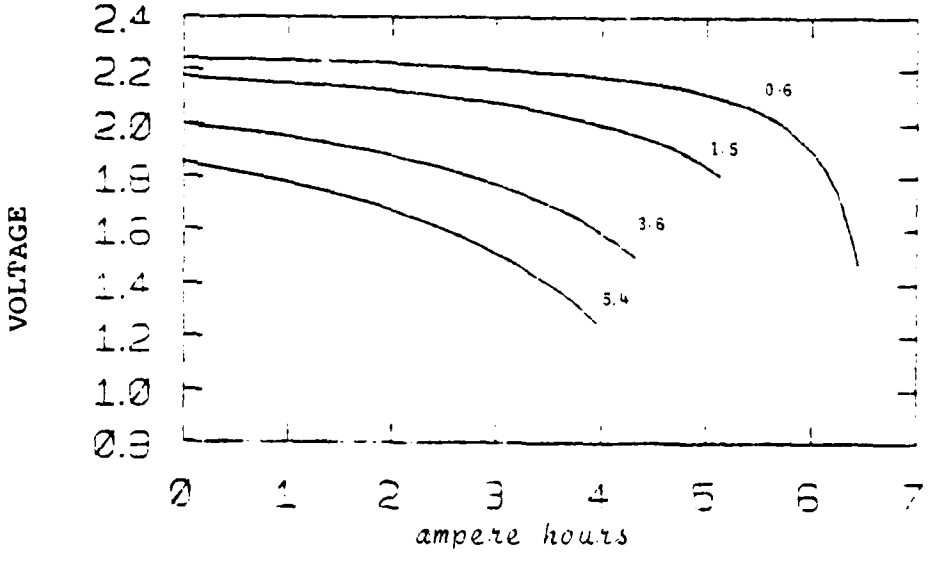

Figure 4-3. Family of Curves for Curve Fit to Shepherd's Equation.

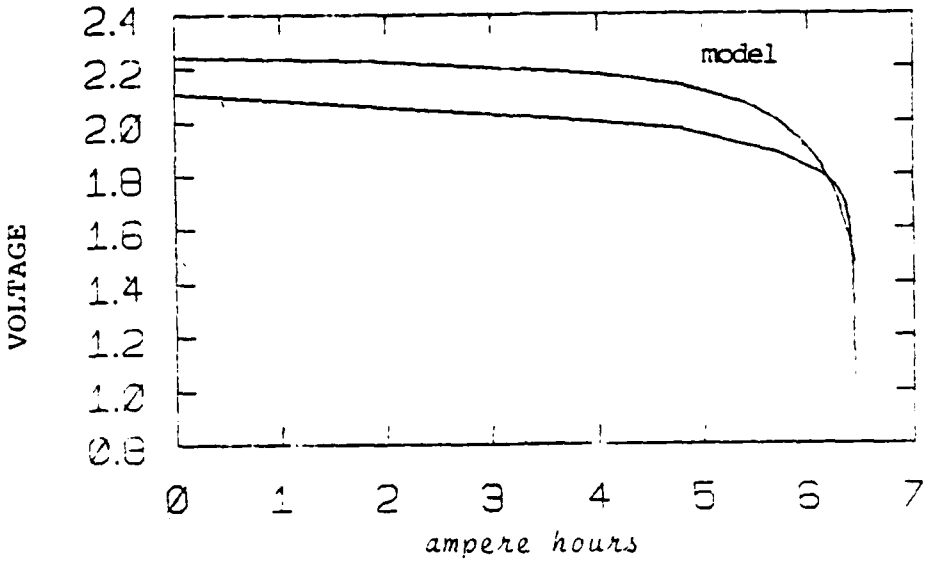

Figure 4-4. 0.6 Amp Discharge Curve and the Modeled Curve for the Fit of the Family of Curves to Shepherd's Equation.

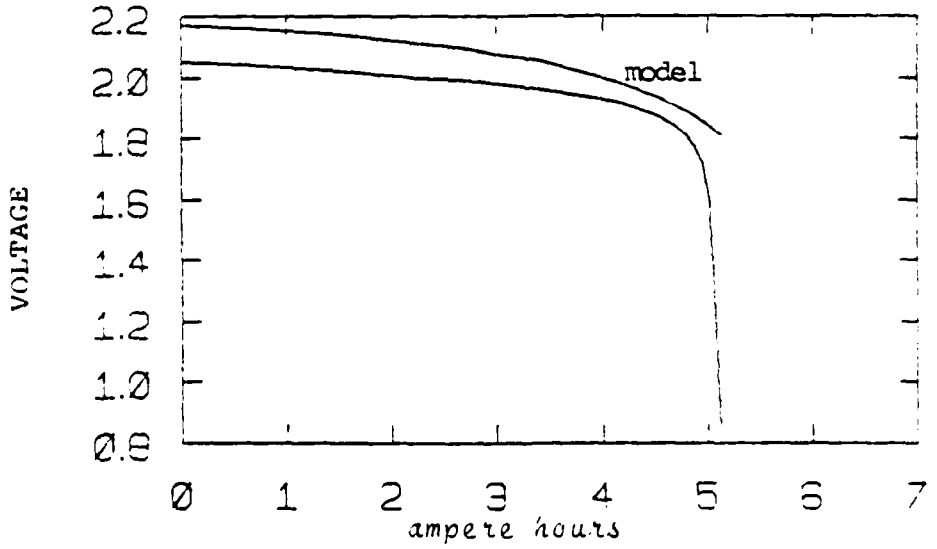

Figure 4-5. 1.5 Amp Discharge Curve and the Modeled Curve for the Fit of the Family of Curves to Shepherd's Equation.

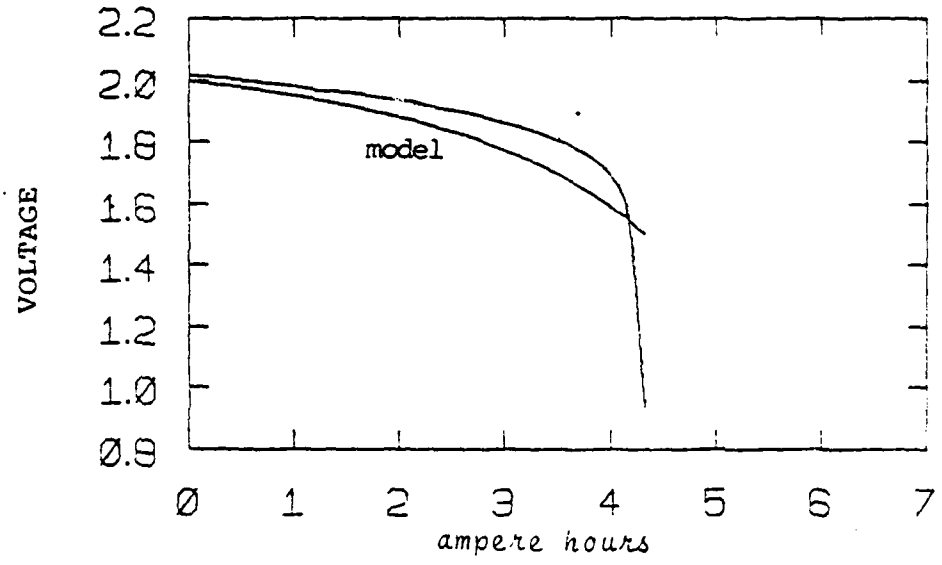

Figure 4-6. 3.6 Amp Discharge Curve and the Modeled Curve for The Fit of the Family of Curves to Shepherd's Equation.

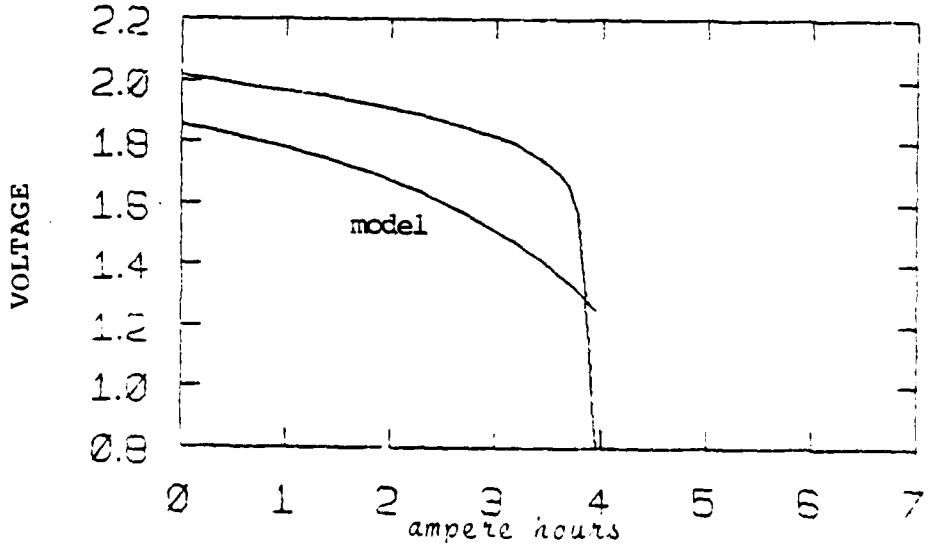

Figure 4-7. 5.4 Amp Discharge Curve and the Modeled Curve for the Fit of the Family of Curves to Shepherd's Equation.

Next, a curve fit for each individual curve was performed using the Shepherd equation. Table 4-1 lists these coefficients with the graphical results shown in figures 4-8 through 4-11.

Current, i	0.6	1.5	3.6	5.4
E_s	2.18	2.18	2.18	2.178
K	0.0137	0.0238	0.0031	0.00142
Q	6.502	5.302	4.373	3.991
R_0	0.2779	0.0481	0.0734	0.05924
Correlation	0.0718	0.1239	0.1585	0.2638

Table 4-1. Curve Fit of Shepherd's Equation to Individual Discharge Curves.

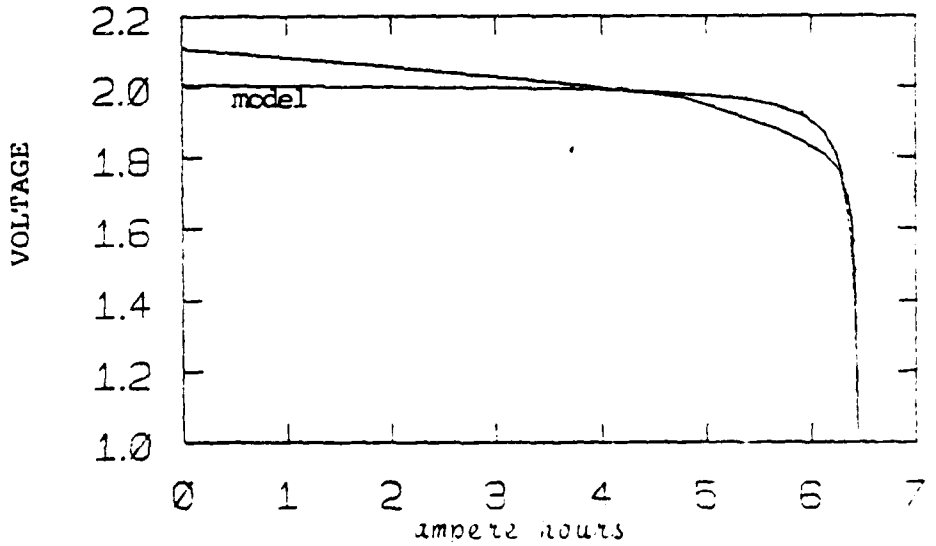

Figure 4-8. 0.6 Amp Discharge Curve and the Modeled Curve for a Fit to the Shepherd Equation of this curve alone.

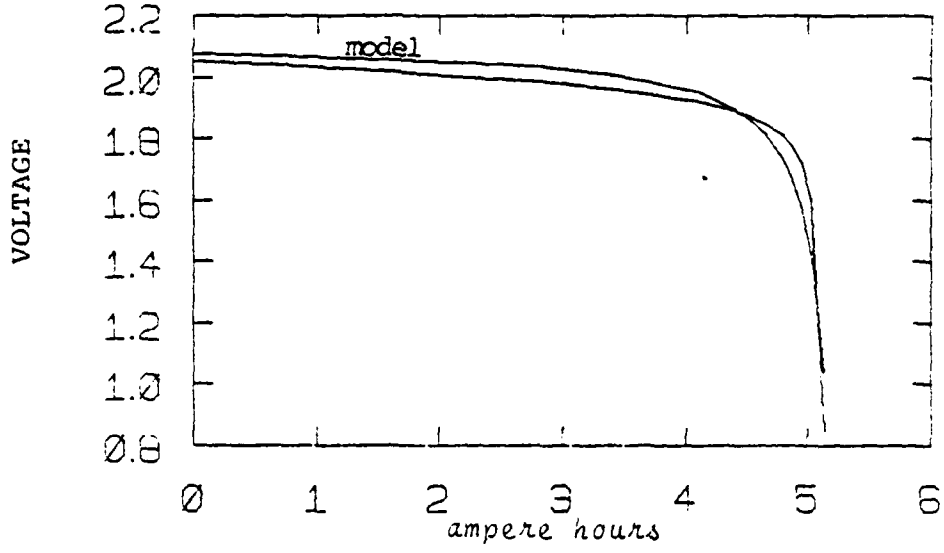

Figure 4-9. 1.5 Amp Discharge Curve and the Modeled Curve for a Fit to the Shepherd Equation of this Curve Alone.

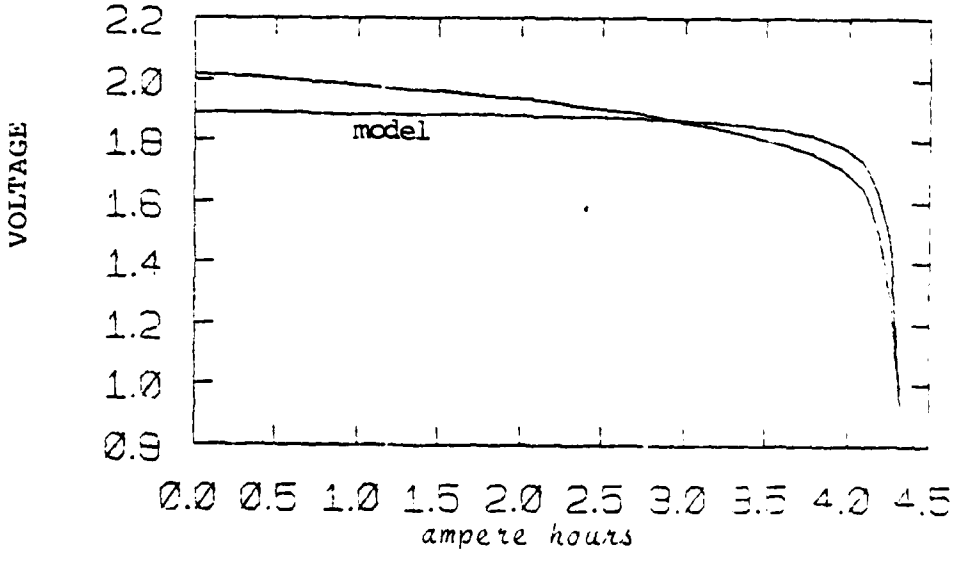

Figure 4-10. 3.6 Amp Discharge Curve and the Modeled Curve for a Fit to the Shepherd Equation of this Curve Alone.

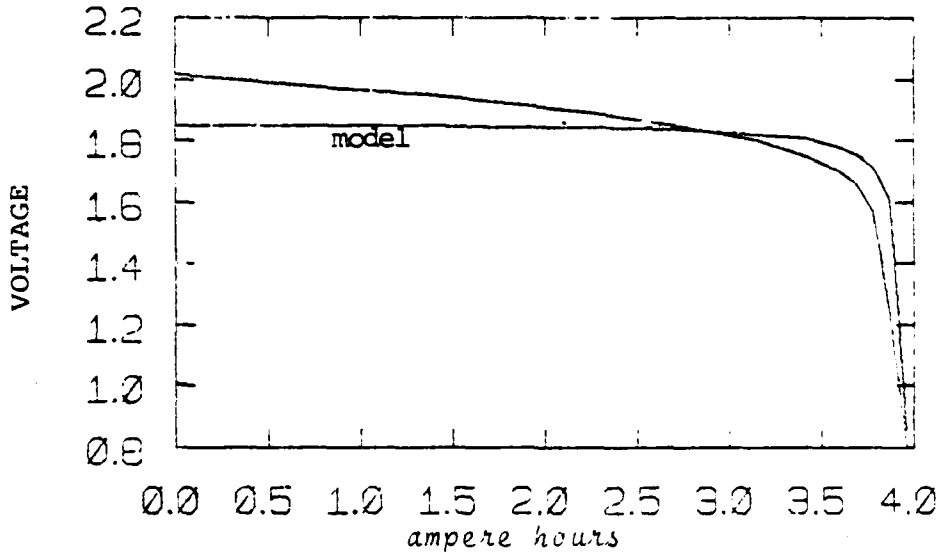

Figure 4-11. 5.4 Amp Discharge Curve and the Modeled Curve for a Fit to the Shepherd Equation of this Curve Alone.

If the slope of the model were adjusted then the correlation between discharge and model would be very good. This suggests modifying the resistance polarization term such that $V_0 = V_0(q,i) = (aq+b)i$. $R_0 = aq+b$ takes into account that the ohmic resistance of the cell changes as the discharge reaction proceeds toward completion. This model simply predicts a linear change in resistance. It may be found that R_0 is also a function of current since the $PbSO_4$ build-up occurs in a different manner at different discharge rates.

The value for Q follows the Peukert equation very well when C and N have the values 5.803 and 1.2227 respectively. Figure 4-12 shows a log-log plot of Q versus I for Peukert's equation.

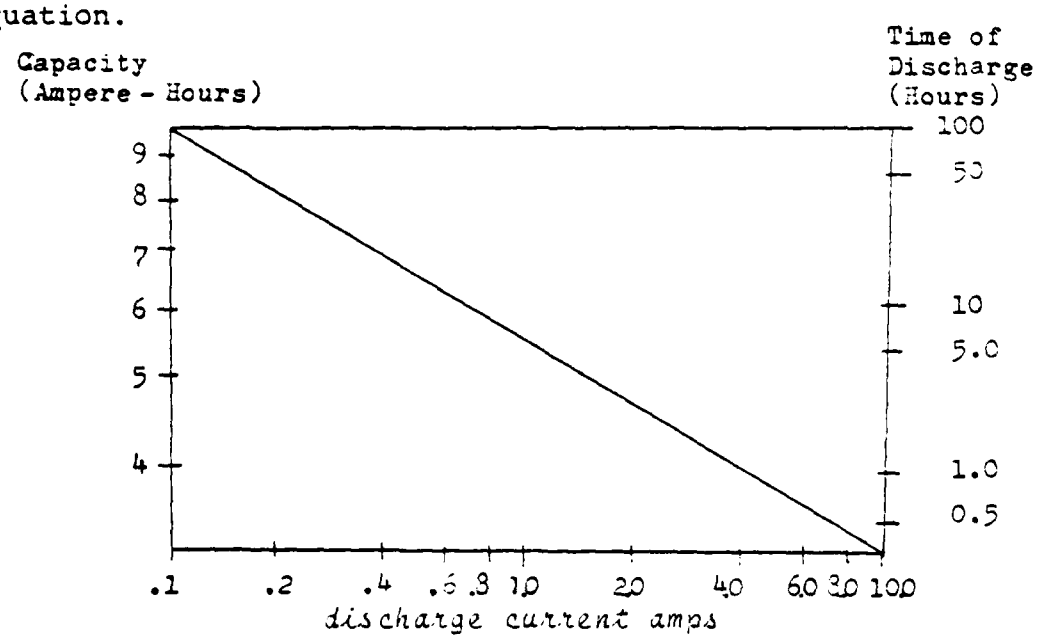

Figure 4-12. Log-Log Plot of Peukert's Equation

$Q = CI^{(1-n)}$ $c = 5.803$ $n = 1.2227$

Modifying the Shepherd Equation by the inclusion of Peukert's capacity model yielded a fit which predicted very well the drop in voltage at the end of discharge. The results obtained did not produce a very good fit to the left of this point, however.

These plots are shown in figures 4-13 through 4-17.

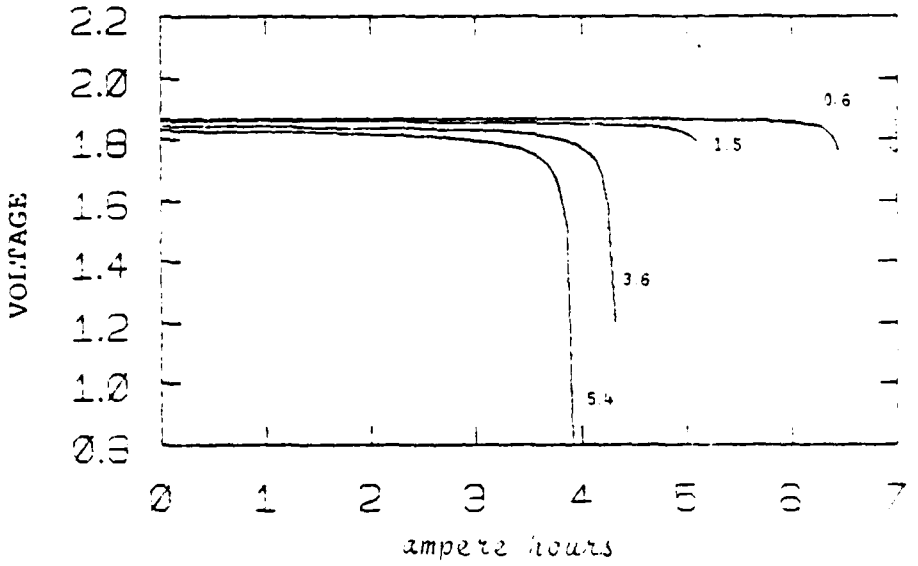

Figure 4-13. Family of Curves for Modification of Capacity Term.

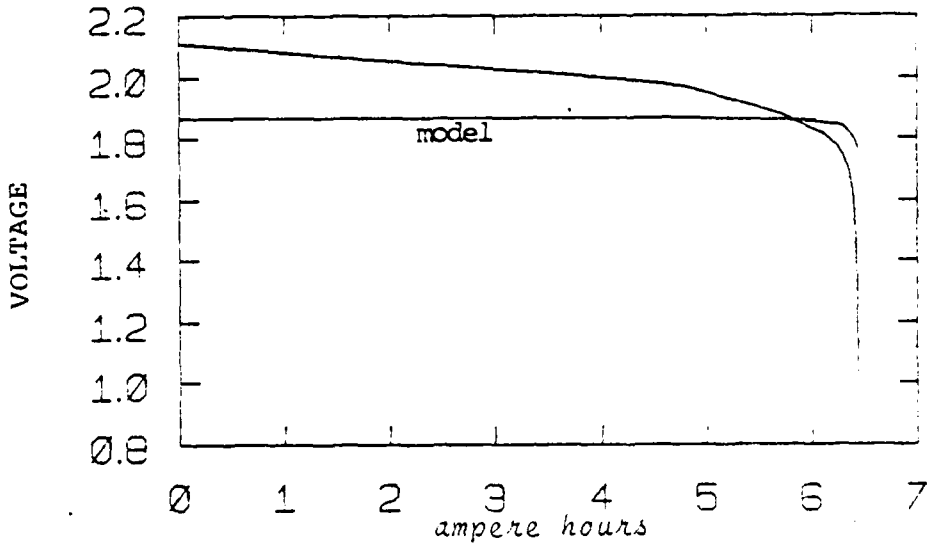

Figure 4-14. 0.6 Amp Fit with Capacity Term Modified.

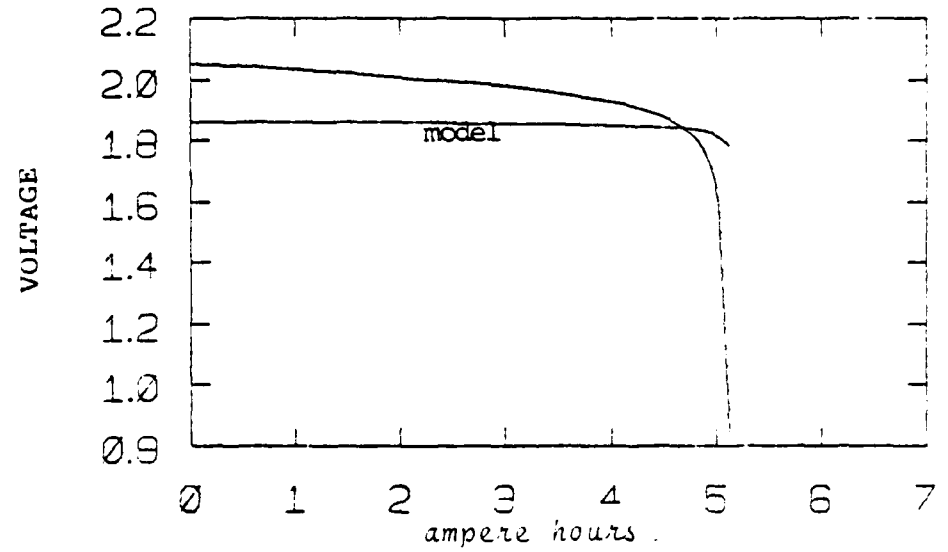

Figure 4-15. 1.5 Amp Fit with Capacity Term Modified.

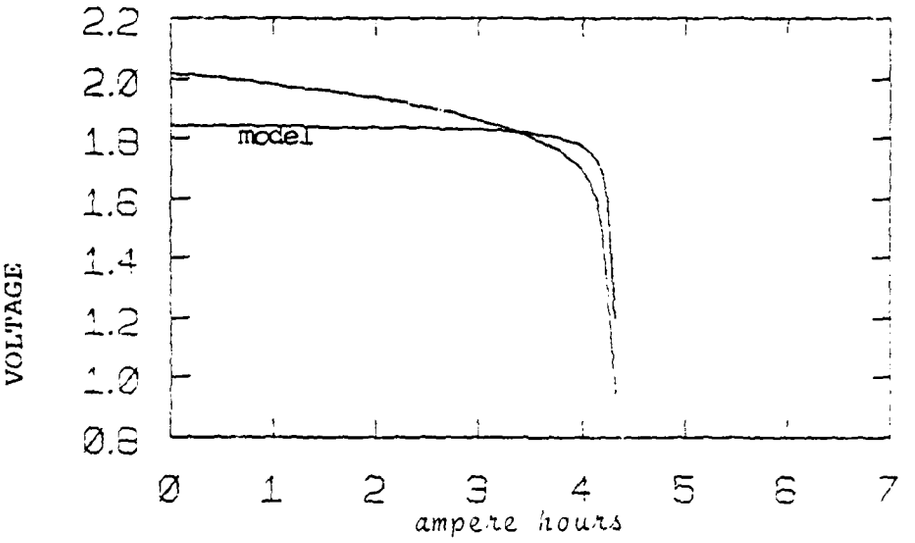

Figure 4-16. 3.6 Amp Fit with Capacity Term Modified.

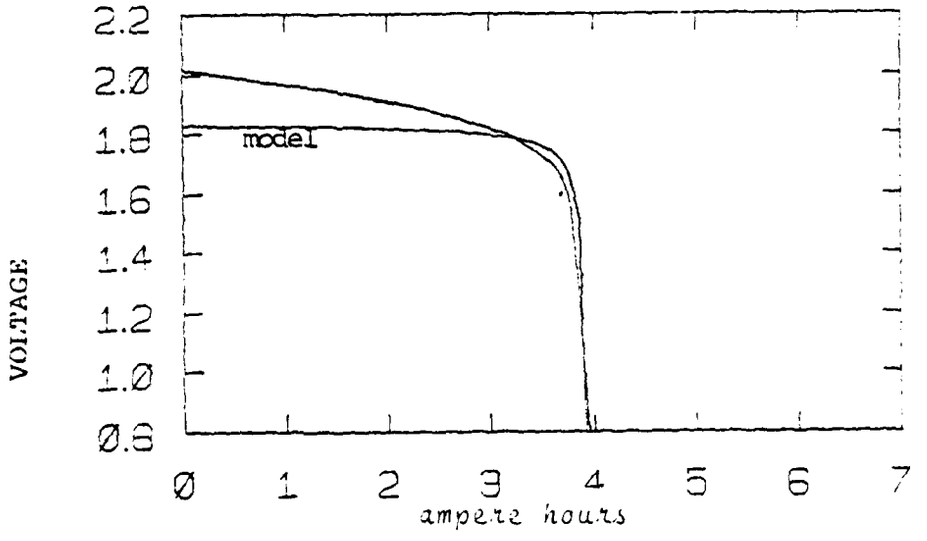

Figure 4-17. 5.4 Amp Fit with Capacity Term Modified.

As mentioned in Section 2.2, the product of K and i, found from the curve fits figures 4-8 through 4-11, tended to be constant, as shown in table 4-2.

i	0.6	1.5	3.6	5.4
K	0.0137	0.0238	0.00310	0.00142
K*i	0.00822	0.0357	0.0112	0.00767

Table 4-2. Comparison of K and the Product K*i.

This suggests that in equation 2.5, $V_d \neq V_d(q,i)$, but rather $V_d = V_d(q) = K \frac{Q}{Q - q}$. By including both this new V_d and capacity terms, the plots of figures 4-18 through 4-22 were produced. These show a definite improvement over previous fits for the family of discharge curves. The values determined were

$$E_s = 2.002$$
$$K = 0.009$$
$$R_0 = 0.03$$

with a correlation of 1.8309.

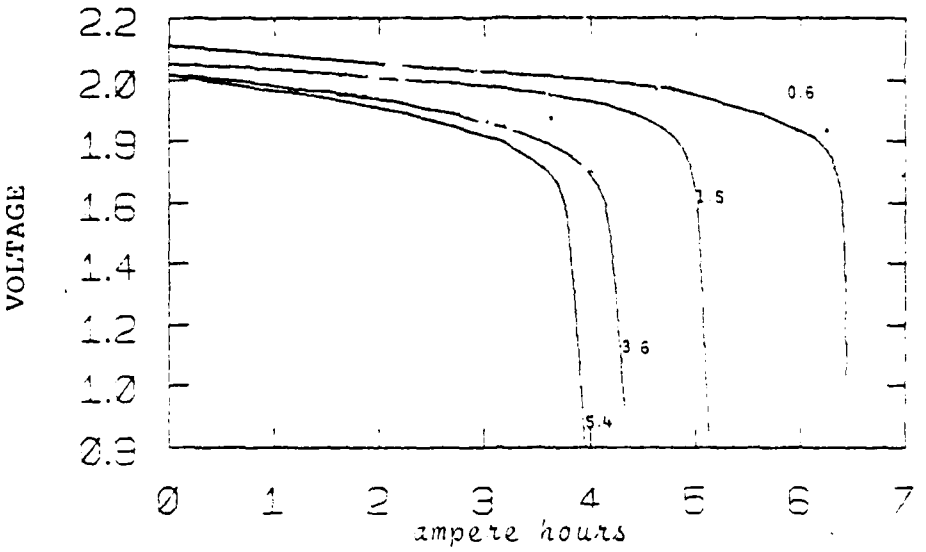

Figure 4-18a. Experimentally Determined Family of Curves

Modification of $V_d = V_d(q)$ and Capacity are shown below:

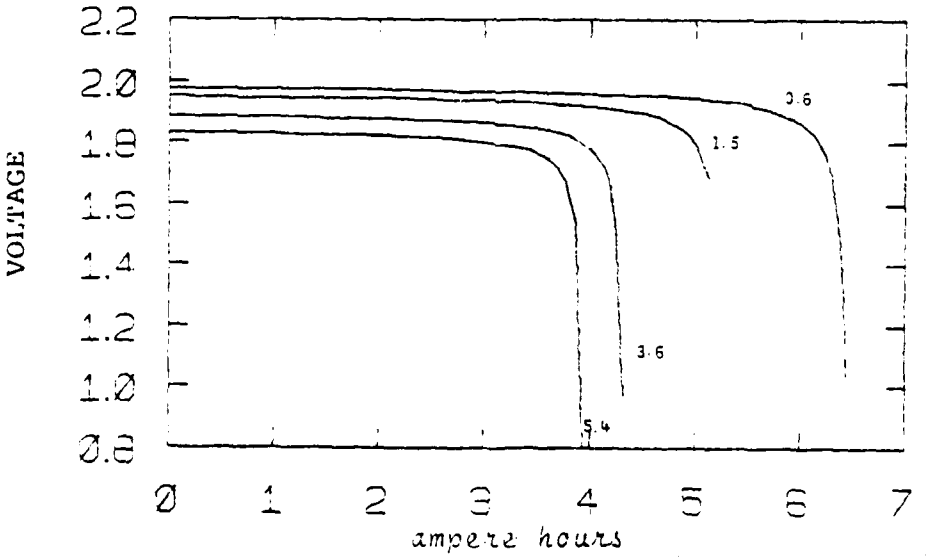

Figure 4-18b. Family of Curves for Modification of $V_d = V_d(q)$ and Capacity.

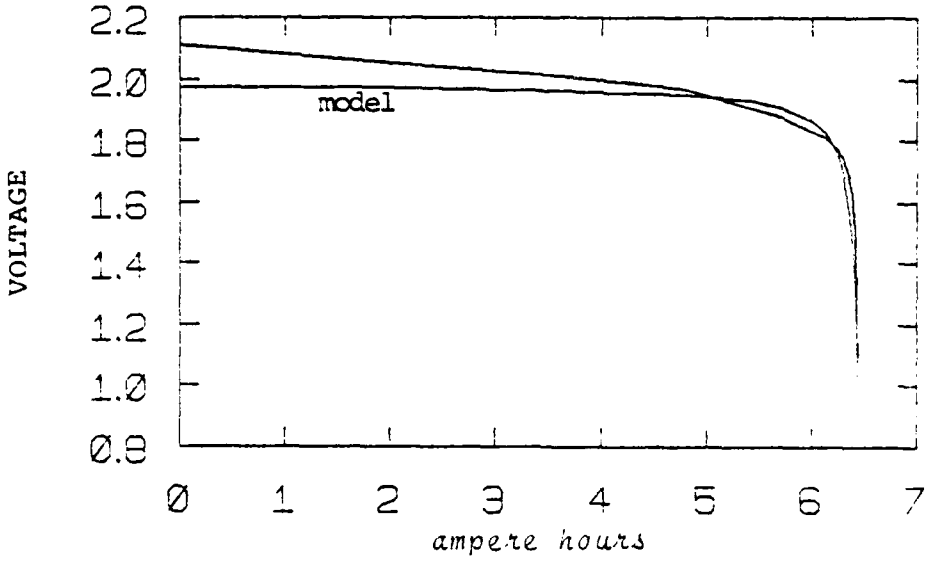

Figure 4-19. 0.6 Amp Fit with Modification of $V_d = V_d(q)$ and Capacity.

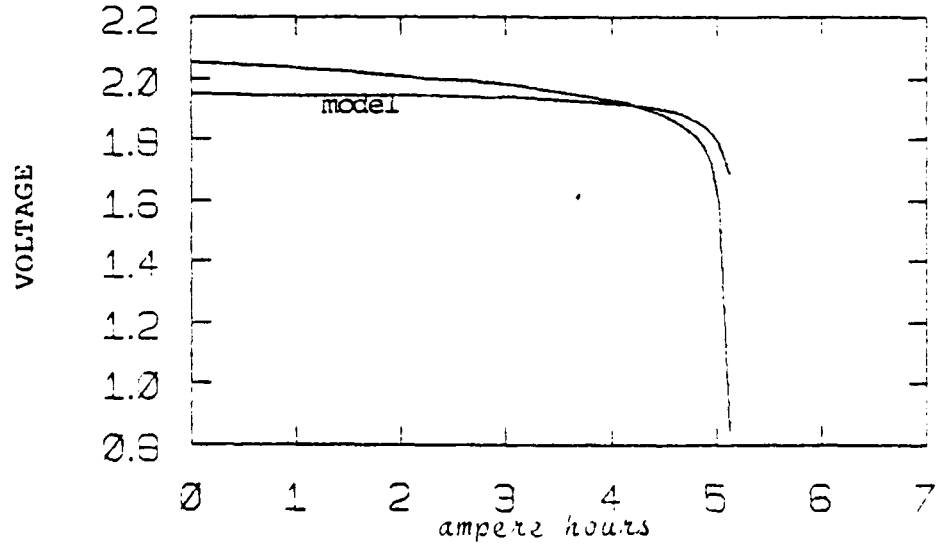

Figure 4-20. 1.5 Amp Fit with Modification of $V_d = V_d(q)$ and Capacity.

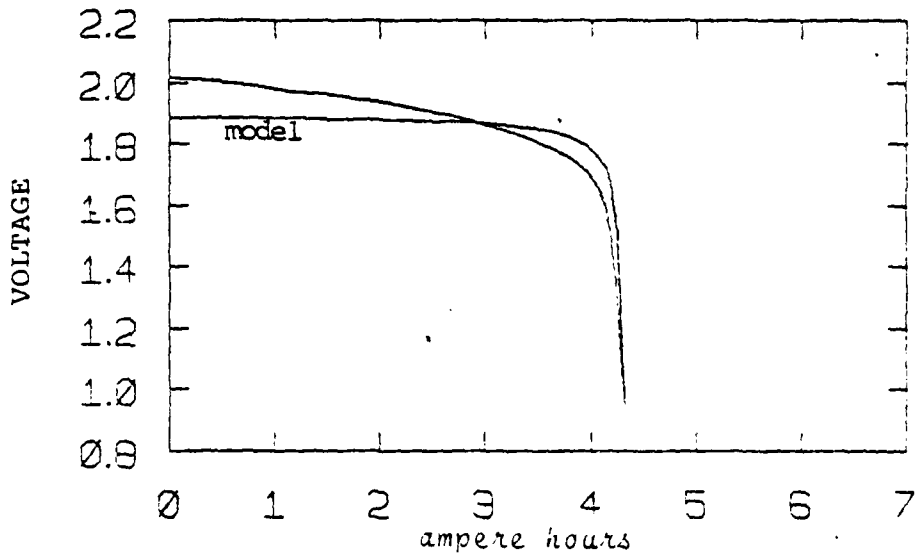

Figure 4-21. 3.6 Amp Fit with Modification of $V_d = V_d(q)$ and Capacity.

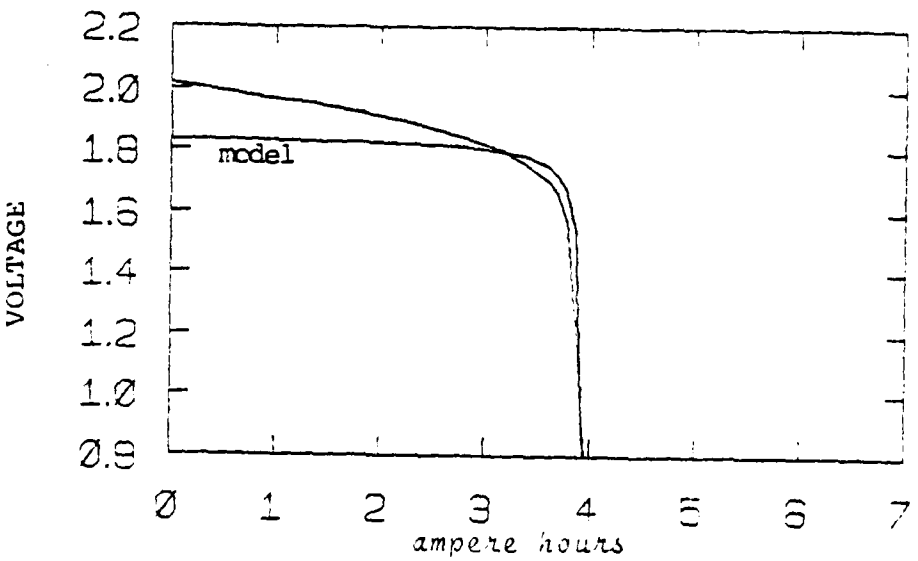

Figure 4-22. 5.4 Amp Fit with Modification of $V_d = V_d(q)$ and Capacity.

Each plot of figures 4-18 through 4-22 suggests that if the ohmic resistance were modeled as a linear function of accumulated charge, a much better fit could be obtained.

Figures 4-23 through 4-26 show the results of individual fits for each discharge curve by modeling

$$R_0 = R_0(q) = R_a q + R_b \ .$$

Table 4-3 lists these results.

i	0.6	1.5	3.6	5.4
E_s	2.180	2.180	2.180	2.180
K	0.00744	0.03453	0.00876	0.00615
R_a	0.1183	0.00073	0.01881	0.01771
R_b	0.03867	0.05424	0.03253	0.02016
Correlation	0.05279	0.12685	0.03129	0.08875
Figure	4-23	4-24	4-25	4-26

Table 4-3. Curve Fit for Individual Discharge Curves with Modifications to Q, V_d, and R_0.

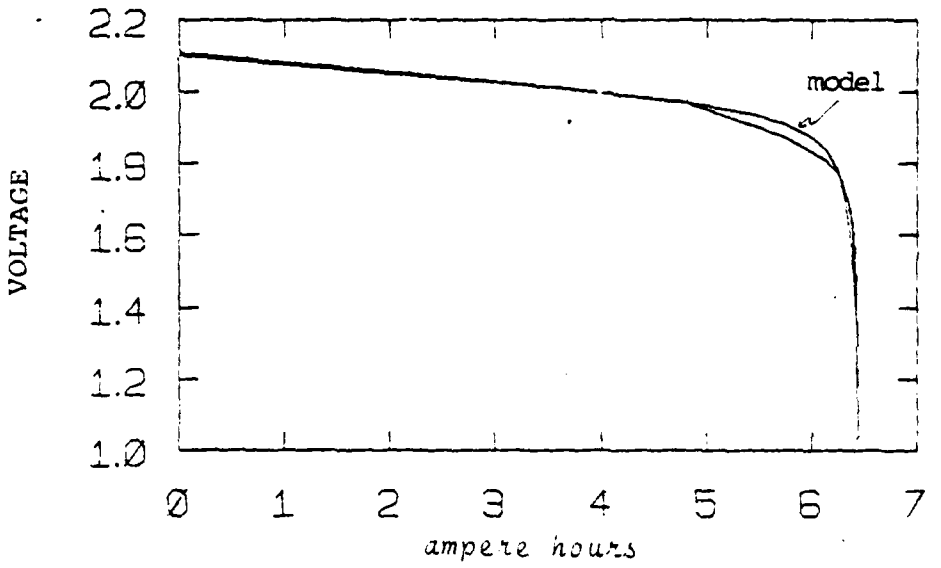

Figure 4-23. Fit of 0.6 Amp Alone for Modification of R_0 and Capacity.

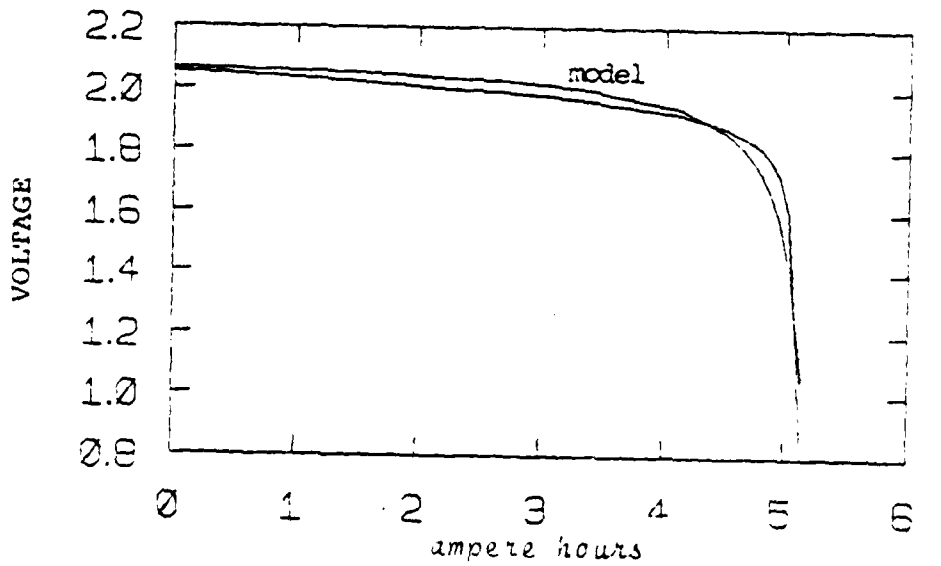

Figure 4-24. Fit of 1.5 Amp Alone for Modification of R_0 and Capacity.

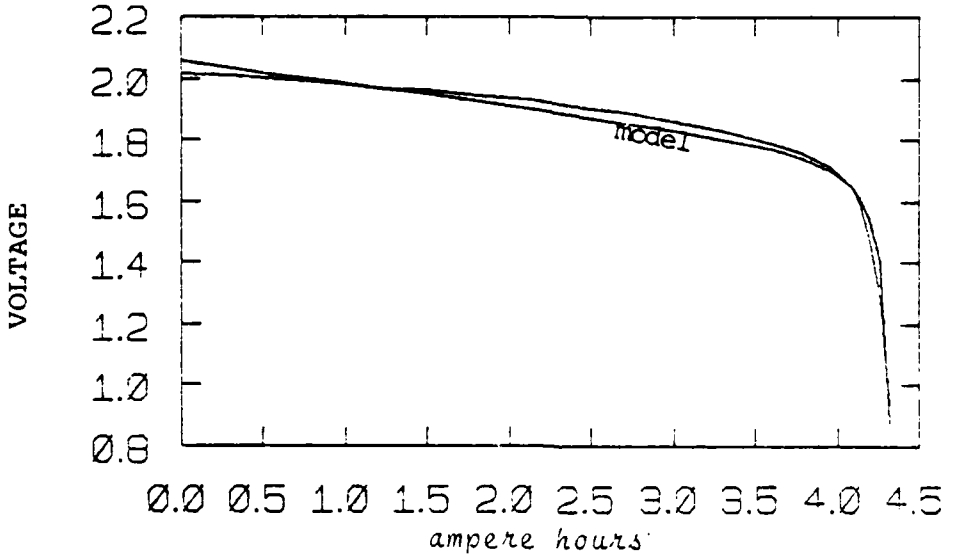

Figure 4-25. Fit of 3.6 Amp Alone for Modification of R_0 and Capacity.

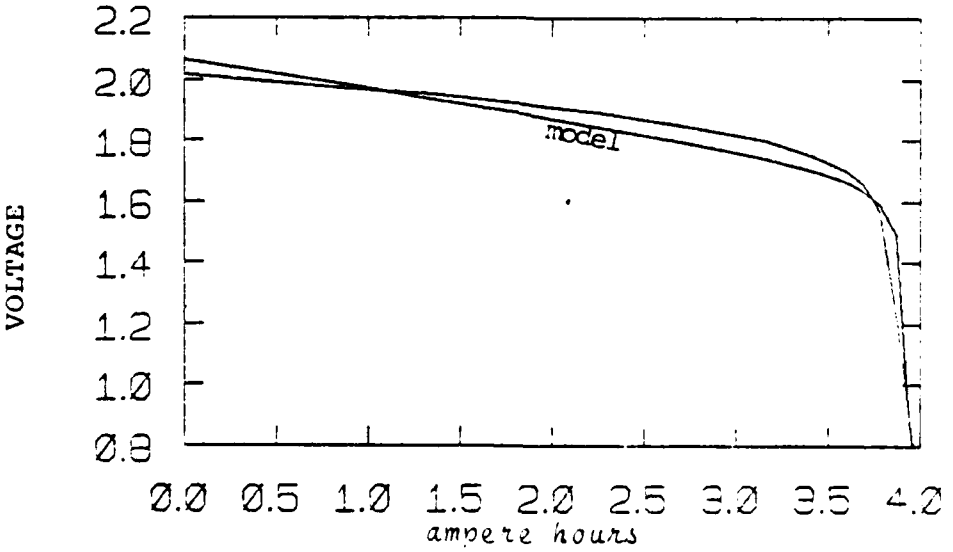

Figure 4-26. Fit of 5.4 Amp Alone for Modification of R_0 and Capacity.

Two more curve fits to the family of discharge curves were performed using the modified ohmic resistance term and Peukert's capacity model.

The first was performed using Shepherd's V_d term with the results shown in figures 4-27 through 4-31. The second fit was made using the modified V_d term. These results are shown in figures 4-32 through 4-36.

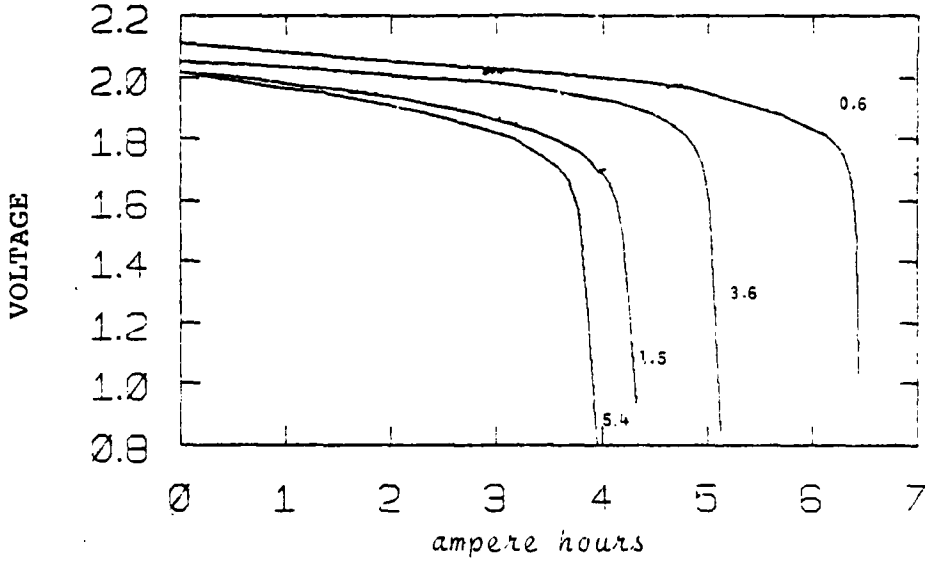

Figure 4-27a. Experimentally Determined Family of Curves

Modification of Capacity and $R_0 = R_0(q)$ are shown below:

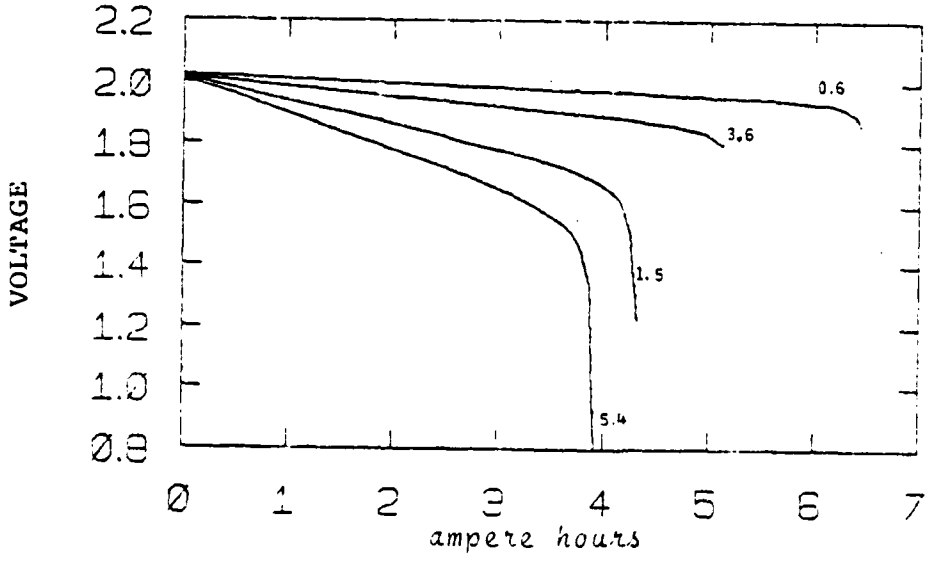

Figure 4-27b. Family of Curves with Modification of Capacity and $R_0 = R_0(q)$.

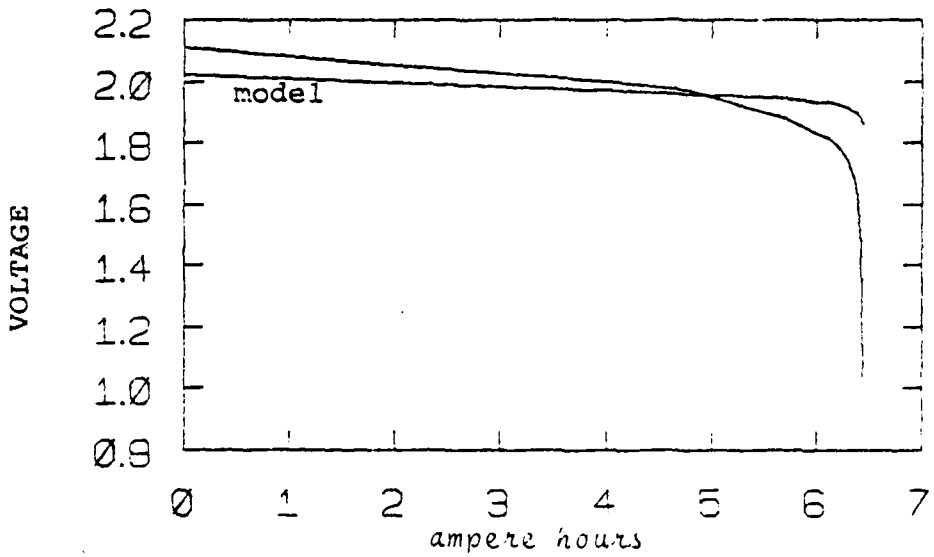

Figure 4-28 0.6 Amp Fit for Modification of R_0 and Capacity.

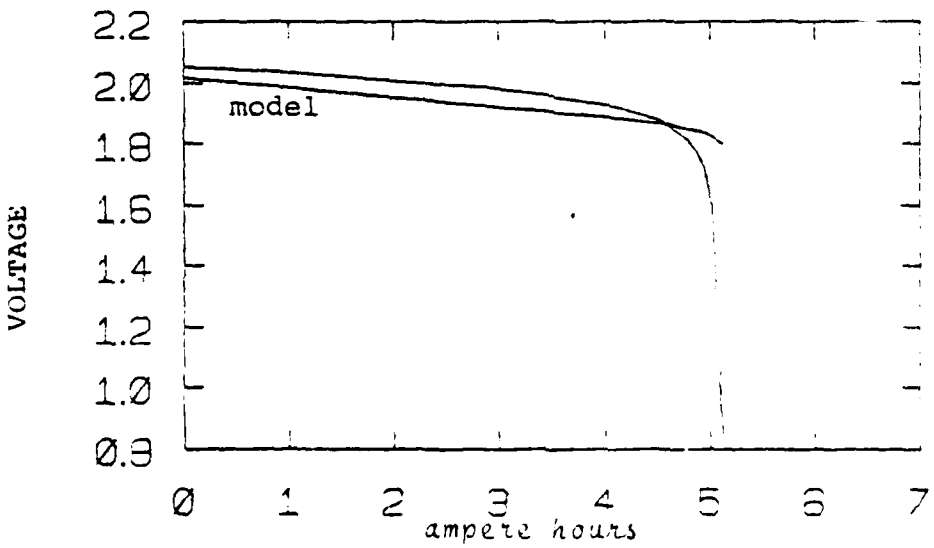

Figure 4-29. 1.5 Amp Fit for Modification of R_0 and Capacity.

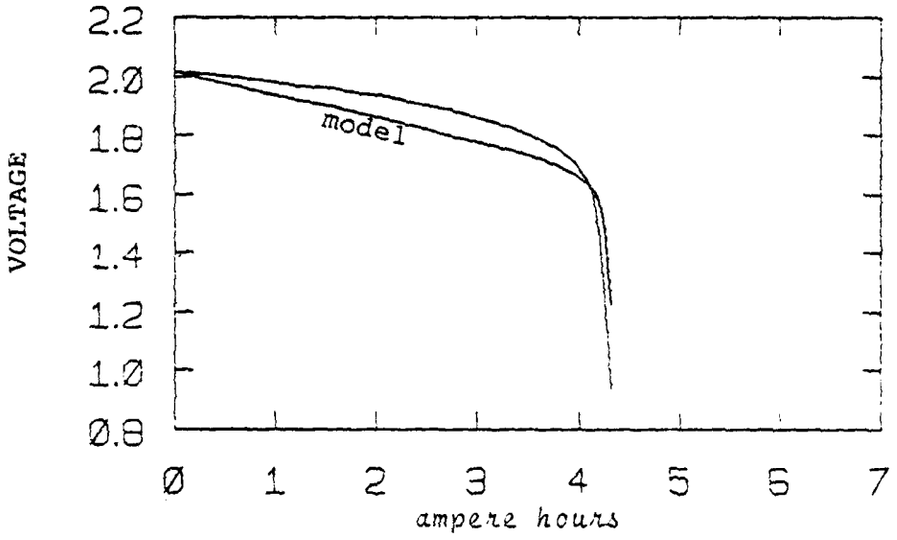

Figure 4-30. 3.6 Amp Fit for Modification of R_0 and Capacity.

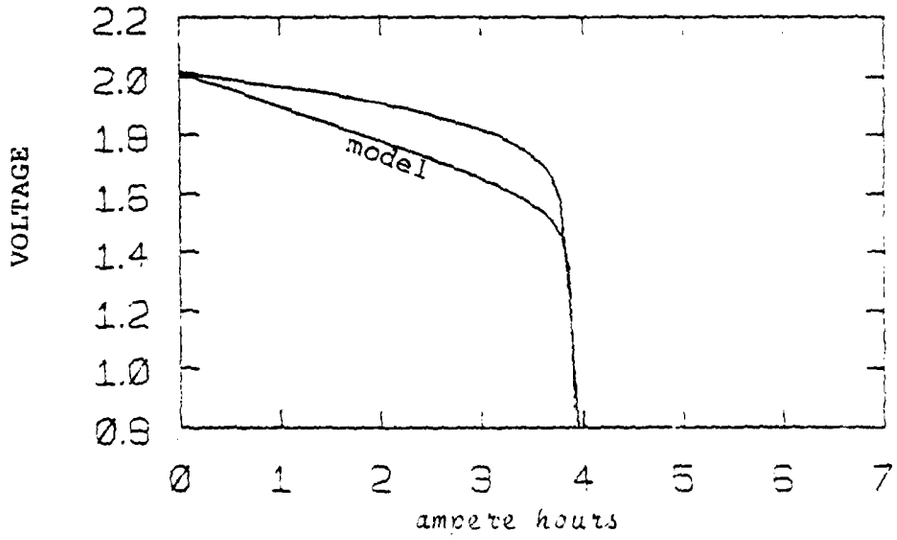

Figure 4-31. 5.4 Amp Fit for Modification of R_0 and Capacity.

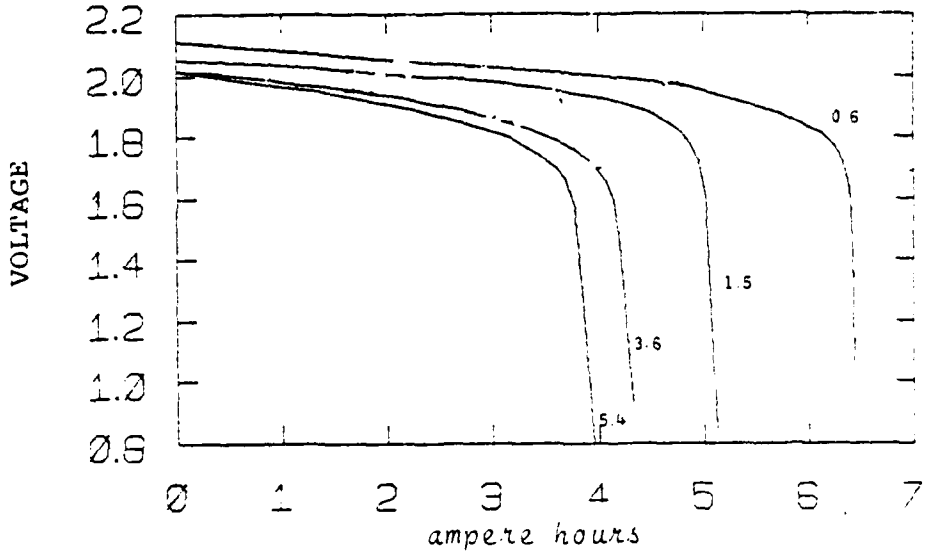

Figure 4-32a. Experimentally Determined Family of Curves

Modifications to V_d, R_0, and Capacity are shown below:

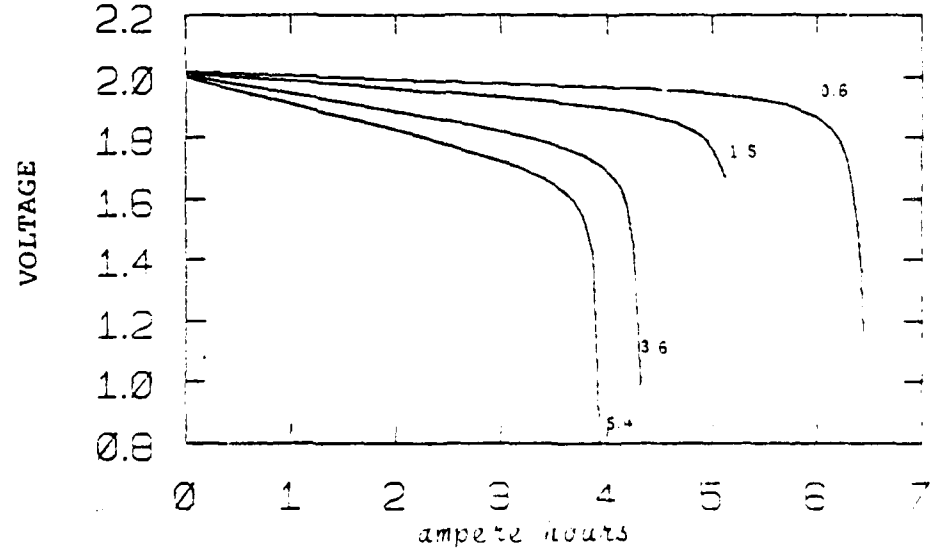

Figure 4-32b. Family of Curves with Modifications to V_d, R_0, and Capacity.

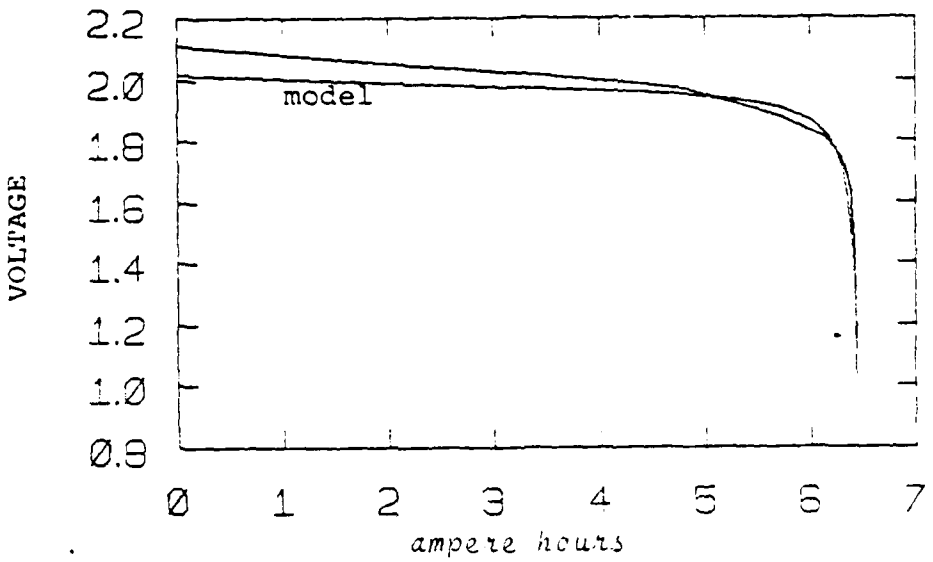

Figure 4-33. 0.6 Amp Curve with Modifications to V_d, R_0, and Capacity.

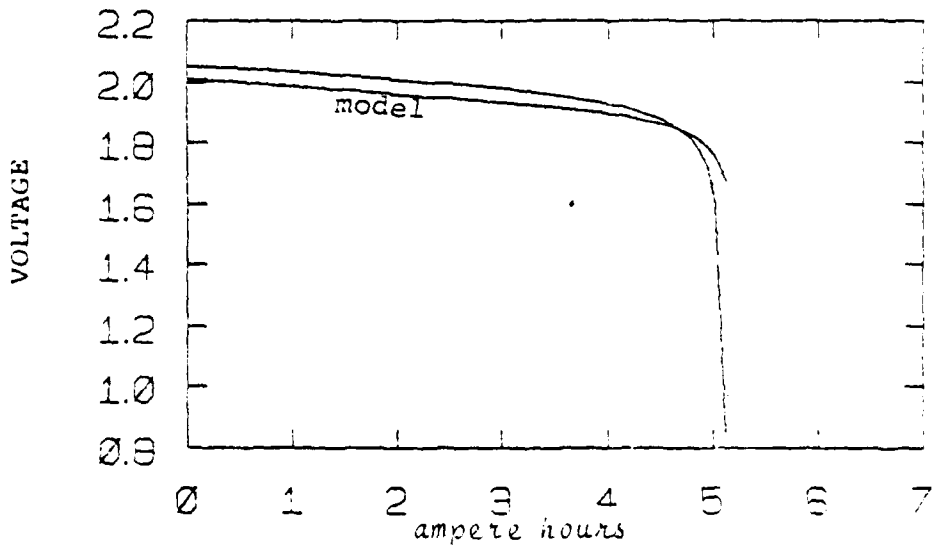

Figure 4-34. 1.5 Amp Curve with Modifications to V_d, R_0, and Capacity.

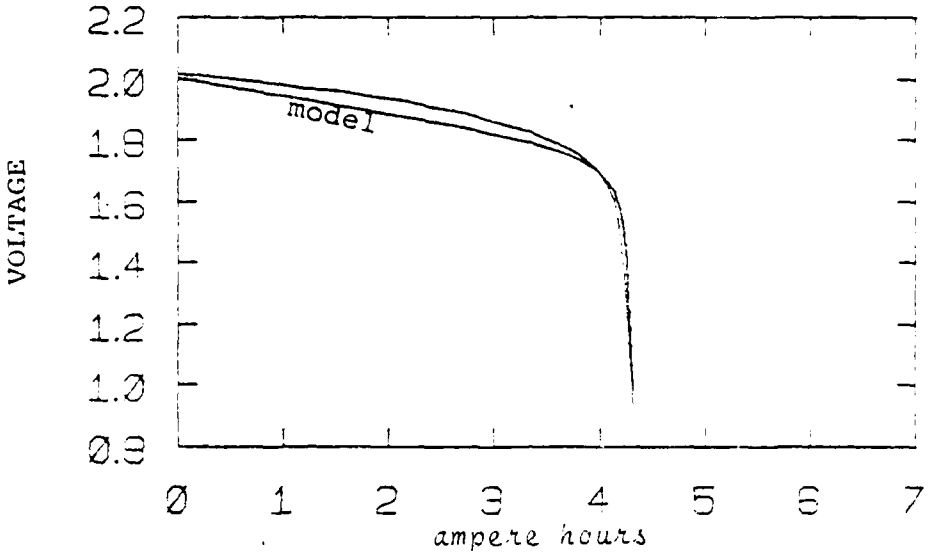

Figure 4-35. 3.6 Amp Curve with Modifications to V_d, R_0, and Capacity.

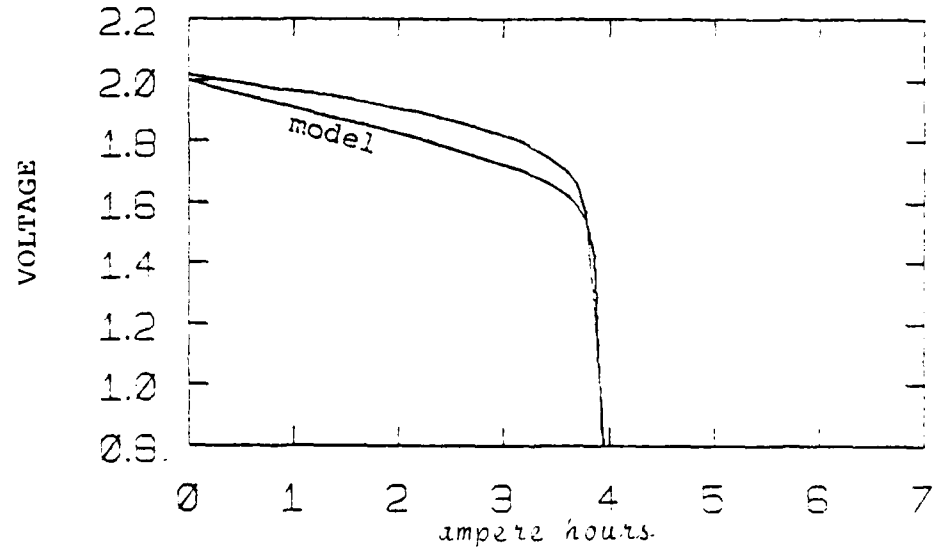

Figure 4-36. 5.4 Amp Curve with Modifications to V_d, R_0, and Capacity.

4.2 LIFE CYCLE TESTING

As was previously mentioned in Section 1.5, according to Bode (1977), the ideal requirement for life testing is that the life test correspond to the load conditions of the battery in the field. However, since ideal testing is impossible due to conditions impossible to duplicate in the laboratory, one must choose another type of test. Kordesch (1977) states that the Cycling Life Test is a test principally to evaluate battery internal components. It does not attempt to simulate car service conditions which are extremely variable. Naturally, this is the type of test chosen for testing the lead-acid battery which was used for experimentation for this thesis.

The life-cycle testing procedure used to determine the change in battery characteristics with age is outlined in Section 3.3. Some of the pertinent data concerning life-cycle testing follows:

Number of Cycles = 135

Time Charge = 193 hours

Time on Discharge = 114 hours

Total number of Ampere Hours Discharged ≅ 375

Amount of Water Lost Due to Hydrolysis = 12ml/cell

To determine changes in cell capacity during the life of the battery several controlled discharges at 3.6 amps were made at different times during the testing. Table 4-4 shows these results. The final capacity was 94% of the previous capacities. Further testing is required to determine the rate at which the capacity decreases.

Number of Prior Cycles	25	91	135
Discharge Time	72	72	67.5
Amphere-hour Capacity	4.32	4.32	4.05

Table 4-4. Capacity Change of Cell #3 During the Life of the Battery.

A great deal of data was generated during the testing but it was considered far to voluminous to be included in its raw form in this report. This data, which is primarily in the form of strip chart recordings, was placed on file with Professor H.M. Paynter at the Massachusetts Institute of Technology.

4.3 UNCERTAINTIES IN EXPERIMENTAL RESULTS

Uncertainties involved in the experimental results were due partly to imperfect knowledge of the state of charge and the inability, at least with the experimental set-up used, to

control certain parameters. The most notable of these was temperature. Variations in temperature have been recognized to produce significant changes in battery characteristics. Great variations in temperature were not encountered since the experiment was performed at room temperature, but there were some variations in this temperature by nearly as much as 10°C. The effect of internal heating at higher discharge rates may have affected results.

The difficulty of knowing the precise state of charge also added a degree of uncertainty. Included in this was the "memory effect," since the amount of preconditioning required to eliminate it was not known.

Also, the knowledge of the mechanism of lead sulfate build-up at the varicus discharge rates was not available.

Due to the differences of the results during curve fitting for the 1.5 amp discharge with respect to the other curves, there was some suspicion that the conditions for that particular discharge may have been different than for the others.

4.4 ADDITIONAL OBSERVATIONS

The method of charging the battery and the point at which charging was terminated was deemed to be the most important factor in placing the battery in the same state-of-charge before the controlled discharges. Figure 4-37 shows a typical constant current charging curve for this experiment.

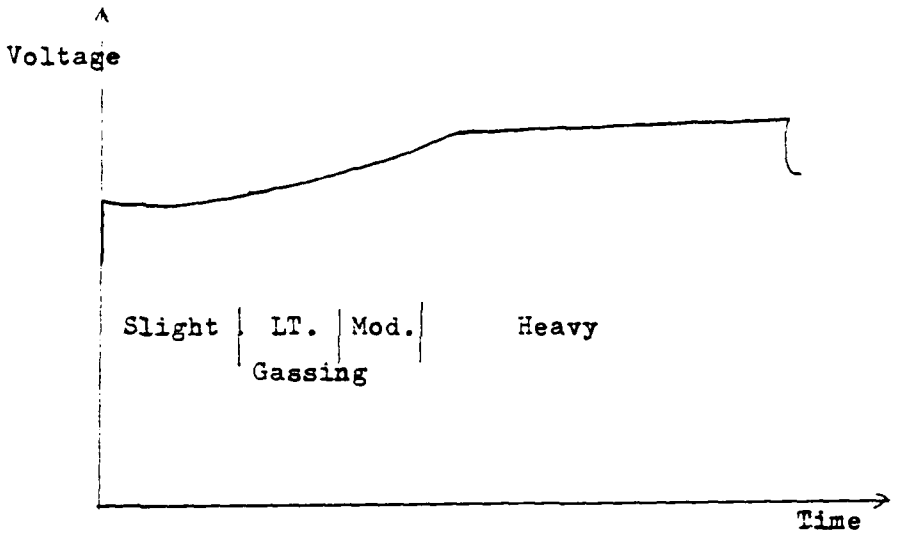

Figure 4-37. Typical Constant Current Charge.

The amount of gassing in the battery was determined by visually observing the amount of gas evolution. The clear battery case was vital in making this determination. By observing the top of the plates from the side of the battery, the following amounts of gassing were determined. Slight gassing was determined when occasional bubbles rose to the surface. This was about the same as when the battery was standing. Light gassing occurred when there was a regular stream of these bubbles rising to the surface. Moderate gassing existed when considerably more activity was observed. This was accompanied on the charging curve by a noticeable increase in the slope. Heavy gassing was typified by a sheet

of small bubbles rising and a generally more violent condition at the surface of the electrolyte. This occurred when the slope of the charge curve reached its maximum and continued throughout overcharging when the voltage stopped increasing.

To obtain equivalent charged conditions, the battery was overcharged when essentially no further increase in voltage occurred at constant current for about 15 to 30 minutes. Most of the energy into the battery at this point went into the hydrolysis of water, indicating that the charge reaction was essentially completed. The observation of the "coup de fouet" after this type of charge and its absense after a partial charge, adds some validity to the degree of completion of the reaction.

An explanation of this phenomenon is that upon initiation of discharge, the electrolyte goes into a meta-stable state, super-saturated with $PbSO_4$, until $PbSO_4$ crystallization sites start to form on the plates. Once this occurs, the voltage recovers from its "dip" and proceeds in a smooth fashion. This recovery was observed to occur after about two minutes. The "coup de fouet" was not observed on a discharge following a partial charge, and was significant for discharges at higher discharge rates, 3.6 and 5.4 amps, which followed a full charge. The magnitude of this dip was approximately 0.01 volt.

When the battery was new, Cell #2 had the lowest capacity. After several days of testing, while moving the experimental

set-up, Cell #3 was inadvertantly placed across a .1Ω resistor. After that occurred, Cell #3 had the lowest capacity and Cell #1 had the greatest.

After all testing was completed, the following observations of the battery were made. The positive plates and connectors had a dark brown color (artist's color "Burnt Umber"), which had a fairly rough appearance. There was some spalling on one edge of one of the plates in cell #3.

The negative plates had a battle-ship grey color. One small piece of material was observed to have broken away from the plate.

There was a fairly uniform coating of sediment in the bottom of the battery. This sludge consisted of two distinct materials. One was a light-colored material with a slightly pinkish tint. The other which uniformly covered the bottom of the battery, and was layered on top of the other sediment, was a dark brown color much the same as the color on the positive plates. The light-colored material may have been white rather than slightly pink because it had been observed by the author et al that the battery case itself seemed to cast the pink tint onto the interior components. It is believed that the light-colored material is actually predominantly $PbSO_4$.

Vinal (1955) states that overcharging produces sludging of a fine brown sediment, and that prolonged undercharging causes

a fine white powder which is principally $PbSO_4$ to be deposited on the bottom. It is felt that the dark brown sediment is PbO_2, which represents a loss of active material from the positive plates. The author notes that prolonged undercharging took place during life-cycle testing.

CHAPTER 5

CONCLUSIONS AND RECOMMENDATIONS

The Shepherd (1965) equation

$$E = E_s - V_d(i,q) - V_0(i) - V_a(q) \tag{5.1}$$

$$V_a(q) = \text{activation polarization} = A \exp \frac{Bq}{Q} \tag{5.2}$$

(neglected due to the short time duration)

$$V_0(i) = \text{ohmic polarization} = R_0 i \tag{5.3}$$

$$V_d(i,q) = \text{diffusion polarization} = K \frac{Q}{Q - q} i \tag{5.4}$$

proved to be an excellent starting point for establishing an electrochemical state model for lead-acid batteries. Using the lead-acid battery of this investigation, the author was able to get a fit to individual discharge curves which required only the modification of the ohmic polarization term (equation 5.3) to the form

$$V_0(i,q) = (R_a q + R_b)\ i. \tag{5.5}$$

in order to get an excellent fit. The results obtained from this fit suggested that a better fit for the family of curves might be obtained by setting K*i constant.

The resulting modified term was

$$V_d(q) = K \frac{Q}{Q - q} . \qquad (5.6)$$

This was the form of the transport polarization suggested by Bode (1977). They also show that the use of the Peukert (1897) capacity model

$$Q(I) = CI^{(1-n)} \qquad (5.7)$$

would predict the rapid drop of voltage at the end of discharge very well.

The modification of the V_d and Q terms seemed valid modeling for the family of discharges, but difficulties were apparent with the ohmic polarization term. There were no particular consistencies in the values of R_a and R_b for the different discharge rates. This may be due to the fact that the buildup of $PbSO_4$ at the plates occurs in a different manner for different discharge rates. Bode (1977) shows that for discharge rates of 6 mA/cm^2 and 1 mA/cm^2 the distribution of $PbSO_4$ throughout the positive, capacity limiting plate, is uniform at full discharge. For current densities of 30 mA/cm^2 and 180 mA/cm^2, there is a lower $PbSO_4$ content at the center of the plate while the content near the surface is the same as

for the lower current densities.

The cell under test had current densities of 3.4, 8.6, 20.7, and 31 mA/cm^2 for discharges of 0.6, 1.5, 3.6, and 5.4A respectively. This suggests that the same mechanisms were encountered in the battery discharge. Since this effect is clearly a function of current, a modification of $V_3(i,q)$ other than that suggested in equation 5.5 may yield a better fit. It may have a form similar to Shepherd's original V_d term, equation 5.4.

Another consideration might be that since equation 5.4 was based on a small current density approximation, another look might be made toward applying equations 2.7 and 2.8 upon which the approximation was based.

A very exciting area of future endeavor, and one which could prove very rewarding, would be the establishment of a model which would predict the family of discharge curves.

Tremendous advancements in the lead-acid battery have been made since the time of Planté and this progress should continue steadily due to the importance of this device in myriad diverse applications. From the standpoint of the System Designer, the establishment of a good state model is a very exciting prospect. This would then allow for a determination of the optimum use of the battery, subject to the constraints of the application.

Further effort in the direction of establishing a model

which would predict the family of discharge curves should include the effect of discharges at various rates during a single cycle. Other effects such as pulsed discharge including both the frequency and duty cycle could then be added.

The inclusion of the prediction of the change in internal characteristics during the secular life of the battery is virtually essential for an optimization. The objective in the design of almost any system is the optimization of a cost (possibly acquisition cost or life cycle cost) subject to various operational criteria. For a system such as an electric vehicle, a very significant cost is the repair cost of battery replacement. Therefore, it is necessary to be able to predict the lowest cost scheme for charge and discharge battery requirments and replacement frequency for various charge/ discharge schemes. To this end, further life cycle testing is recommended.

To produce applicable results, it is felt by the author that all cycles should be identical except those due to secular changes in the battery. A rather sophisticated control system needs to be developed. All charges and discharges should be conducted at constant current. During charge, a significant period on overcharge is recommended to ensure that the state-of-charge is nearly identical prior to any discharge. Since the amount of overcharge cannot be determined by sensing the voltage level alone, some means needs to be devised to deter-

mine the slope of the voltage curve and to control the time on charge at this level. It is also recommended that a single cell be used during testing to eliminate any effects from the other cells.

An attempt has been made throughout this thesis to draw conclusions on the suitability of the Shepherd (1965) equation as a state model for lead-acid batteries. Modifications to this equation were proposed, among them was the modeling of the ohmic polarization as a linear function of accumulated charge to obtain a good fit to a single discharge curve. These curves revealed the interesting result that the product K*I was nearly constant. Also, Peukert's equation was used to model the cell capacity.

The difficulties encountered in the attempt to obtain an optimum state model have been evaluated and enumerated. However, new discoveries about the lead-acid battery are being made, and new technology may supply the means to overcome the difficulties. Almost certainly, economic, ecological, sociological and technological problems with our current energy resources will dictate to society the necessity of assessing the place of the lead-acid battery in our future.

BIBLIOGRAPHY

REFERENCE BOOKS

Bode, H., Lead-Acid Batteries, John Wiley, New York, 1977.

Kordesch, K.V., Batteries, Vol. 2, Marcel Dekker, New York, 1977.

Millman, J., and Taub, J., Pulse, Digital, and Switching Waveforms, McGraw-Hill, New York, 1965.

Vinal, C.W., Storage Batteries, 4th ed., John Wiley, New York, 1955.

REFERENCES

Baikie, P.E., Gillibrand, M.I., and Peters, K., Electrochim, Acta, 17, 839 (1972).

Bode, H., Electrotechn. Z., 18, 857 (1966).

Davytan, O.K., Bull. Acad. USSR (1946), 737.

Gladstone, J.H. and Tribe, A., Nature, 25, 221, 461; 26, 251, 342, 602; 27, 583, (1882-1883).

Liebenow, C., Dissertation Gottingen 1905, Z. Elektrochem. 4, 58-63, (1897).

Peukert, W., Elektr. Techn. Z. 18 (1897), 287-288.

Rabl, M., Z. Elektrochem. 42, (1936), 114-120.

Schröder, L., Electrotechn. 12 (1894), 587.

Shepherd, C.M., J. Electrochem. Soc. 112 (1965), 657-664.

AD-A110 892 MASSACHUSETTS INST OF TECH CAMBRIDGE F/G 7/4
ELECTROCHEMICAL STATE MODELS OF LEAD-ACID BATTERIES.(U)
MAY 79 R J PFISTER

UNCLASSIFIED NL

2 OF 2
AD A
110892

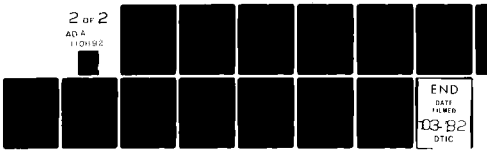

END
DATE FILMED
03-82
DTIC

APPENDIX A

NUMERIC DATA CORRESPONDING TO FIGURE 4-1.

0.6 Amp Disch		1.5 Amp Disch		3.6 Amp Disch		5.4 Amp Disch	
Ah	Volt (exp)	Ah	Volt (exp)	Ah	Volt (exp)	Ah	Volt (exp)
0.00	2.110	0.00	2.080	0.00	2.000	0.00	1.930
1.80	2.060	0.75	2.040	0.36	2.010	0.45	1.900
3.60	2.010	1.50	2.020	0.60	2.000	0.90	1.870
4.20	1.990	2.25	2.000	0.90	1.990	1.35	1.940
4.80	1.970	2.63	1.990	1.20	1.970	1.80	1.820
5.40	1.910	3.00	1.980	1.50	1.940	2.25	1.690
5.70	1.880	3.38	1.930	1.80	1.940	2.70	1.480
6.00	1.930	4.13	1.910	2.10	1.930	3.15	1.790
6.12	1.910	4.50	1.890	2.40	1.910	3.42	1.750
6.24	1.770	4.65	1.840	2.70	1.880	3.60	1.700
6.30	1.740	4.80	1.810	3.00	1.840	3.64	1.660
6.34	1.690	4.88	1.770	3.30	1.850	3.78	1.370
6.38	1.630	4.95	1.720	3.50	1.790	3.87	1.230
6.40	1.470	5.03	1.600	3.72	1.750	3.96	0.900
6.44	1.030	5.10	1.100	3.96	1.710		
		5.13	0.850	4.08	1.650		
				4.14	1.590		
				4.20	1.480		
				4.26	1.280		
				4.32	0.940		

Numeric data corresponding to Figures 4-4 and 4-5

Coefficients for the Model

E_s	K	Q	R_o	Corr
2.295	0.08086	6.844	0.0092	3.5008

0.6 Amp Discharge

Ah	Volt (Exp)	Volt (Eqn)	Diff
0.00	2.110	2.246	0.136
1.80	2.060	2.228	0.168
3.60	2.010	2.192	0.182
4.20	1.990	2.169	0.179
4.80	1.970	2.132	0.162
5.40	1.910	2.064	0.154
5.70	1.880	2.004	0.124
6.00	1.830	1.901	0.071
6.12	1.810	1.836	0.026
6.24	1.770	1.745	-0.025
6.30	1.740	1.684	-0.056
6.36	1.690	1.605	-0.085
6.39	1.630	1.563	-0.067
6.42	1.470	1.511	0.041
6.44	1.030	1.473	0.443

1.5 Amp Discharge

Ah	Volt (Exp)	Volt (Eqn)	Diff
0.00	2.050	2.170	0.120
0.75	2.040	2.157	0.117
1.50	2.020	2.139	0.119
2.25	2.000	2.113	0.113
2.63	1.990	2.087	0.097
3.00	1.980	2.077	0.097
3.38	1.960	2.084	0.124
4.13	1.920	1.988	0.068
4.50	1.880	1.939	0.059
4.65	1.850	1.915	0.065
4.80	1.810	1.887	0.077
4.88	1.770	1.872	0.102
4.95	1.720	1.855	0.135
5.03	1.600	1.637	0.037
5.10	1.100	1.817	0.717
5.13	0.850	1.810	0.960

Numeric data corresponding to Figures 4-6 and 4-7.

Coefficients for the Model

E_s	K	Q	R_o	Corr
2.295	0.08086	6.844	0.0092	3.5008

3.6 Amp Discharge

Ah	Volt (Exp)	Volt (Eqn)	Diff
0.00	2.017	2.000	-0.017
0.30	2.010	1.987	-0.023
0.60	2.000	1.972	-0.028
0.90	1.984	1.956	-0.028
1.20	1.970	1.938	-0.032
1.50	1.960	1.919	-0.041
1.80	1.945	1.896	-0.049
2.10	1.930	1.871	-0.059
2.40	1.910	1.843	-0.067
2.70	1.890	1.811	-0.079
3.00	1.860	1.773	-0.087
3.30	1.830	1.729	-0.101
3.60	1.790	1.677	-0.113
3.78	1.760	1.641	-0.119
3.96	1.710	1.601	-0.109
4.08	1.650	1.571	-0.079
4.14	1.590	1.555	-0.035
4.20	1.490	1.538	0.048
4.26	1.260	1.320	0.060
4.32	0.940	1.502	0.562

5.4 Amp Discharge

Ah	Volt (Exp)	Volt (Eqn)	Diff
0.00	2.014	1.853	-0.161
0.45	1.990	1.809	-0.181
0.90	1.970	1.797	-0.173
1.35	1.950	1.746	-0.204
1.80	1.920	1.697	-0.223
2.25	1.890	1.639	-0.251
2.70	1.850	1.[illegible]	-0.[illegible]
3.15	1.800	1.481	-0.319
3.42	1.750	1.417	-0.333
3.60	1.700	1.369	-0.331
3.69	1.660	1.342	-0.318
3.78	1.570	1.314	-0.256
3.87	1.[illegible]	1.[illegible]	[illegible]
3.96	0.830	1.284	1.454

Numeric Data corresponding to Figures 4-8 and 4-9.

Coefficients for the model.

See table 4-1

0.6 Amp Discharge

Ah	Volt (Exp)	Volt (Eqn)	Diff
0.00	2.110	2.005	-0.105
1.80	2.060	2.002	-0.058
3.60	2.010	1.995	-0.015
4.20	1.990	1.990	0.000
4.80	1.970	1.982	0.012
5.40	1.910	1.965	0.055
5.70	1.880	1.947	0.067
6.00	1.830	1.907	0.077
6.12	1.810	1.873	0.063
6.24	1.770	1.809	0.039
6.30	1.740	1.748	0.008
6.36	1.690	1.635	-0.054
6.39	1.630	1.555	-0.075
6.42	1.470	1.761	-0.109
6.44	1.030	1.150	0.120

1.5 Amp Discharge

Ah	Volt (Exp)	Volt (Eqn)	Diff
0.00	2.052	2.070	0.020
0.75	2.040	2.036	0.006
1.50	2.020	2.059	0.039
2.25	2.000	2.045	0.045
2.63	1.980	2.007	0.027
3.00	1.960	2.006	0.046
3.38	1.960	2.017	0.057
4.13	1.920	1.947	0.027
4.50	1.880	1.870	-0.009
4.65	1.850	1.818	-0.032
4.80	1.810	1.731	-0.079
4.88	1.770	1.663	-0.106
4.95	1.720	1.570	-0.150
5.03	1.600	1.425	-0.175
5.10	1.100	1.171	0.071
5.13	0.850	1.038	0.188

Numeric data corresponding to figures 4-10 and 4-11

Coefficients for the Model

See Table 4-1

3.6 Amp Discharge

Ah	Volt (Exp)	Volt (Eqn)	Diff
0.00	2.017	1.890	-0.127
0.30	2.010	1.889	-0.121
0.60	2.000	1.888	-0.112
0.90	1.984	1.887	-0.097
1.20	1.970	1.885	-0.085
1.50	1.960	1.884	-0.076
1.80	1.945	1.882	-0.063
2.10	1.930	1.879	-0.051
2.40	1.910	1.876	-0.034
2.70	1.890	1.872	-0.018
3.00	1.860	1.865	0.005
3.30	1.830	1.855	0.025
3.60	1.790	1.838	0.048
3.78	1.760	1.819	0.059
3.96	1.710	1.783	0.073
4.08	1.650	1.734	0.084
4.14	1.590	1.691	0.101
4.20	1.480	1.619	0.139
4.26	1.290	1.469	0.179
4.32	0.940	0.980	0.040

5.4 Amp Discharge

Ah	Volt (Exp)	Volt (Eqn)	Diff
0.00	2.014	1.850	-0.164
0.45	1.990	1.840	-0.141
0.90	1.970	1.848	-0.122
1.35	1.950	1.847	-0.103
1.80	1.920	1.844	-0.076
2.25	1.890	1.841	-0.049
2.70	1.850	1.834	-0.016
3.15	1.800	1.822	0.022
3.42	1.750	1.805	0.055
3.60	1.700	1.790	0.090
3.69	1.650	1.756	0.106
3.78	1.570	1.713	0.143
3.87	1.230	1.505	0.275
3.96	0.800	0.871	0.071

Numeric Data corresponding to Figures 4-14 and 4-15.

COEFFICIENTS FOR THE MODEL

E_s	K	C	n	Corr	R_o
1.872	0.00177	5.803	1.22270	3.19808	0.00651

0.6 Amp Discharge

Ah	Volt (Exp)	Volt (Eqn)	Diff
0.00	2.110	1.867	-0.243
1.80	2.060	1.957	-0.103
3.60	2.010	1.866	-0.144
4.20	1.990	1.865	-0.125
4.80	1.970	1.864	-0.106
5.40	1.910	1.862	-0.048
5.70	1.880	1.859	-0.021
6.00	1.880	1.854	0.024
6.12	1.810	1.850	0.040
6.24	1.770	1.842	0.072
6.30	1.740	1.834	0.094
6.36	1.690	1.819	0.129
6.39	1.630	1.806	0.176
6.42	1.470	1.784	0.314
6.44	1.030	1.757	0.727

1.5 Amp Discharge

Ah	Volt (Exp)	Volt (Eqn)	Diff
0.00	2.052	1.860	-0.192
0.75	2.040	1.859	-0.181
1.50	2.020	1.859	-0.161
2.25	2.000	1.858	-0.142
2.63	1.990	1.857	-0.133
3.00	1.980	1.856	-0.124
3.38	1.968	1.855	-0.113
4.13	1.920	1.850	-0.070
4.50	1.880	1.845	-0.035
4.65	1.850	1.841	-0.009
4.80	1.810	1.834	0.024
4.88	1.770	1.829	0.059
4.95	1.720	1.822	0.102
5.03	1.600	1.811	0.211
5.10	1.100	1.792	0.692
5.13	0.850	1.783	0.933

Numeric Data corresponding to figures 4-16 and 4-17

COEFFICIENTS FOR THE MODEL

E_s	K	C	n	Corr	R_o
1.872	0.00177	5.803	1.22270	3.19808	0.00651

3.6 Amp Discharge

Ah	Volt (Exp)	Volt (Eqn)	Diff
0.00	2.017	1.842	-0.175
0.30	2.010	1.842	-0.168
0.60	2.000	1.841	-0.159
0.90	1.984	1.841	-0.143
1.20	1.970	1.840	-0.130
1.50	1.960	1.839	-0.121
1.80	1.945	1.838	-0.107
2.10	1.930	1.836	-0.094
2.40	1.910	1.834	-0.076
2.70	1.890	1.832	-0.058
3.00	1.860	1.828	-0.032
3.30	1.830	1.822	-0.008
3.60	1.790	1.812	0.022
3.78	1.760	1.801	0.041
3.96	1.710	1.780	0.070
4.09	1.650	1.750	0.100
4.14	1.590	1.724	0.134
4.20	1.480	1.678	0.198
4.25	1.280	1.578	0.298
4.32	0.940	1.197	0.257

5.4 Amp Discharge

Ah	Volt (Exp)	Volt (Eqn)	Diff
0.00	2.014	1.827	-0.187
0.45	1.990	1.826	-0.164
0.90	1.970	1.825	-0.145
1.35	1.950	1.822	-0.128
1.80	1.920	1.819	-0.101
2.25	1.890	1.815	-0.075
2.70	1.850	1.807	-0.043
3.15	1.800	1.791	-0.009
3.42	1.750	1.779	0.029
3.60	1.700	1.738	0.038
3.69	1.660	1.708	0.048
3.78	1.570	1.652	0.082
3.87	1.230	1.509	0.279
3.96	0.800	1.372	0.572

Numeric Data corresponding to Figures 4-19 and 4-20.

COEFFICIENTS FOR THE MODEL.

E_s	K	C	n	Corr	R_o
2.002	0.00900	5.803	1.22270	1.83086	0.03006

0.6 Amp Discharge

Ah	Volt (Exp)	Volt (Eqn)	Diff
0.00	2.110	1.975	-0.135
1.80	2.060	1.972	-0.088
3.60	2.010	1.964	-0.046
4.20	1.990	1.959	-0.031
4.80	1.970	1.950	-0.020
5.40	1.910	1.931	0.021
5.70	1.880	1.911	0.031
6.00	1.830	1.867	0.037
6.12	1.810	1.831	0.021
6.24	1.770	1.761	-0.009
6.30	1.740	1.694	-0.046
6.36	1.690	1.572	-0.118
6.39	1.630	1.461	-0.169
6.42	1.470	1.270	-0.200
6.44	1.030	1.040	0.010

1.5 Amp Discharge

Ah	Volt (Exp)	Volt (Eqn)	Diff
0.00	2.052	1.948	-0.104
0.75	2.040	1.946	-0.094
1.50	2.020	1.944	-0.076
2.25	2.000	1.941	-0.059
2.63	1.990	1.939	-0.051
3.00	1.980	1.936	-0.044
3.38	1.968	1.932	-0.036
4.13	1.920	1.916	-0.004
4.50	1.890	1.907	0.017
4.65	1.858	1.894	0.036
4.80	1.810	1.860	0.050
4.88	1.770	1.845	0.075
4.95	1.720	1.821	0.101
5.03	1.660	1.785	0.125
5.10	1.100	1.720	0.620
5.13	0.850	1.687	0.837

Numeric data corresponding to Figures 4-21 and 4-22.

COEFFICIENTS FOR THE MODEL

E_s	K	C	n	Corr	R_o
2.002	0.00900	5.803	1.22270	1.83086	0.03006

3.6 Amp Discharge

Ah	Volt (Exp)	Volt (Eqn)	Diff
0.00	2.017	1.885	-0.132
0.30	2.010	1.884	-0.126
0.60	2.000	1.883	-0.117
0.90	1.984	1.882	-0.102
1.20	1.970	1.881	-0.089
1.50	1.960	1.880	-0.080
1.80	1.945	1.879	-0.067
2.10	1.930	1.876	-0.054
2.40	1.910	1.874	-0.036
2.70	1.896	1.870	-0.026
3.00	1.860	1.865	0.005
3.30	1.830	1.857	0.027
3.60	1.790	1.842	0.052
3.78	1.760	1.826	0.066
3.96	1.710	1.796	0.086
4.08	1.650	1.755	0.105
4.14	1.590	1.717	0.127
4.20	1.480	1.652	0.172
4.26	1.280	1.511	0.231
4.32	0.940	0.974	0.034

5.4 Amp Discharge

Ah	Volt (Exp)	Volt (Eqn)	Diff
0.00	2.014	1.821	-0.193
0.45	1.980	1.820	-0.160
0.90	1.970	1.828	-0.142
1.35	1.950	1.826	-0.124
1.80	1.920	1.823	-0.097
2.25	1.890	1.819	-0.071
2.70	1.850	1.812	-0.038
3.15	1.800	1.797	-0.003
3.42	1.750	1.776	0.026
3.60	1.700	1.747	0.047
3.69	1.660	1.719	0.059
3.78	1.570	1.666	0.096
3.87	1.230	1.530	0.300
3.96	0.000	0.460	-0.340

Numeric data corresponding to Figures 4-23 and 4-24.

COEFFICIENTS FOR THE MODEL

SEE TABLE 4-3.

0.6 Amp Discharge

Ah	Volt (Exp)	Volt (Eqn)	Diff
0.00	2.110	2.102	-0.008
1.80	2.060	2.057	-0.003
3.60	2.010	2.009	-0.001
4.20	1.990	1.991	0.001
4.80	1.970	1.969	-0.001
5.40	1.910	1.940	0.030
5.70	1.880	1.916	0.036
6.00	1.830	1.873	0.043
6.12	1.810	1.840	0.030
6.24	1.770	1.780	0.010
6.30	1.740	1.723	-0.017
6.36	1.690	1.621	-0.069
6.39	1.630	1.529	-0.101
6.42	1.470	1.370	-0.100
6.44	1.030	1.180	0.150

1.5 Amp Discharge

Ah	Volt (Exp)	Volt (Eqn)	Diff
0.00	2.052	2.064	0.012
0.75	2.040	2.058	0.018
1.50	2.020	2.049	0.029
2.25	2.000	2.036	0.036
2.63	1.990	2.027	0.037
3.00	1.980	2.016	0.036
3.38	1.965	2.000	0.037
4.13	1.920	1.939	0.019
4.50	1.880	1.865	-0.015
4.65	1.850	1.813	-0.037
4.80	1.810	1.729	-0.081
4.88	1.770	1.664	-0.106
4.95	1.720	1.573	-0.147
5.03	1.600	1.432	-0.168
5.10	1.100	1.196	0.096
5.13	0.850	1.05[illegible]	0.20[illegible]

Numeric data corresponding to Figures 4-25 and 4-26.

COEFFICIENTS FOR THE MODEL

SEE TABLE 4-3.

3.6 Amp Discharge

Ah	Volt (Exp)	Volt (Eqn)	Diff
0.00	2.017	2.054	0.037
0.30	2.010	2.033	0.023
0.60	2.000	2.012	0.012
0.90	1.984	1.991	0.007
1.20	1.970	1.970	0.000
1.50	1.960	1.948	-0.012
1.80	1.945	1.926	-0.019
2.10	1.930	1.904	-0.026
2.40	1.910	1.881	-0.029
2.70	1.890	1.857	-0.033
3.00	1.860	1.832	-0.028
3.30	1.830	1.804	-0.026
3.60	1.790	1.769	-0.021
3.78	1.760	1.741	-0.019
3.96	1.710	1.700	-0.010
4.08	1.650	1.652	0.002
4.14	1.590	1.611	0.021
4.20	1.480	1.524	0.044
4.26	1.280	1.402	0.122
4.32	0.940	0.875	-0.065

5.4 Amp Discharge

Ah	Volt (Exp)	Volt (Eqn)	Diff
0.00	2.014	2.005	-0.009
0.45	1.990	2.001	0.011
0.90	1.970	1.977	0.007
1.35	1.950	1.933	-0.017
1.80	1.920	1.888	-0.032
2.25	1.890	1.842	-0.048
2.70	1.850	1.794	-0.056
3.15	1.800	1.741	-0.059
3.42	1.750	1.701	-0.049
3.60	1.700	1.663	-0.037
3.69	1.660	1.635	-0.025
3.78	1.570	1.591	0.021
3.87	1.230	1.490	0.260
3.96	0.800	0.750	-0.050

Numeric data corresponding to Figures 4-28 and 4-29.

COEFFICIENTS FOR THE MODEL

E_s	K	C	n	Corr	R_a	R_b
2.020	0.00128	5.303	1.22270	3.05102	0.02100	0.00022

0.6 Amp Discharge

Ah	Volt (Exp)	Volt (Eqn)	Diff
0.00	2.110	2.019	-0.091
1.80	2.060	1.996	-0.064
3.60	2.010	1.973	-0.037
4.20	1.990	1.965	-0.025
4.80	1.970	1.957	-0.013
5.40	1.910	1.948	0.038
5.70	1.880	1.942	0.062
6.00	1.830	1.935	0.105
6.12	1.810	1.930	0.120
6.24	1.770	1.923	0.153
6.30	1.740	1.916	0.176
6.36	1.690	1.905	0.215
6.39	1.630	1.895	0.265
6.42	1.470	1.878	0.408
6.44	1.030	1.859	0.829

1.5 Amp Discharge

Ah	Volt (Exp)	Volt (Eqn)	Diff
0.00	2.052	2.018	-0.034
0.75	2.040	1.994	-0.046
1.50	2.020	1.970	-0.050
2.25	2.000	1.946	-0.054
2.63	1.990	1.934	-0.056
3.00	1.980	1.921	-0.059
3.38	1.963	1.908	-0.055
4.13	1.920	1.881	-0.039
4.50	1.900	1.866	-0.034
4.65	1.850	1.858	0.008
4.80	1.810	1.848	0.038
4.88	1.770	1.843	0.073
4.95	1.720	1.835	0.115
5.03	1.600	1.825	0.225
5.10	1.100	1.809	0.709
5.13	0.950	1.801	0.851

Numeric Data corresponding to Figures 4-30 and 4-31.

COEFFICIENTS FOR THE MODEL

E_s	K	C	n	Corr	R_a	R_b
2.020	0.00128	5.803	1.22270	3.05102	0.02100	0.00022

3.6 Amp Discharge

Ah	Volt (Exp)	Volt (Eqn)	Diff
0.00	2.017	2.015	-0.002
0.30	2.010	1.992	-0.018
0.60	2.000	1.969	-0.031
0.90	1.984	1.946	-0.038
1.20	1.970	1.923	-0.047
1.50	1.960	1.899	-0.061
1.80	1.945	1.876	-0.069
2.10	1.930	1.852	-0.078
2.40	1.910	1.828	-0.082
2.70	1.890	1.803	-0.087
3.00	1.860	1.778	-0.082
3.30	1.830	1.751	-0.079
3.60	1.790	1.721	-0.069
3.78	1.760	1.699	-0.061
3.96	1.710	1.670	-0.040
4.08	1.650	1.640	-0.010
4.14	1.590	1.616	0.026
4.20	1.480	1.578	0.098
4.26	1.280	1.502	0.222
4.32	0.940	1.222	0.282

5.4 Amp Discharge

Ah	Volt (Exp)	Volt (Eqn)	Diff
0.00	2.014	2.012	-0.002
0.45	1.990	1.960	-0.030
0.90	1.970	1.928	-0.042
1.35	1.950	1.896	-0.054
1.80	1.920	1.802	-0.118
2.25	1.890	1.748	-0.142
2.70	1.850	1.692	-0.158
3.15	1.800	1.629	-0.171
3.42	1.750	1.603	-0.147
3.60	1.700	1.540	-0.160
3.69	1.660	1.508	-0.152
3.78	1.570	1.457	-0.113
3.87	1.230	1.343	0.113
3.96	0.900	0.810	-0.090

Numeric data corresponding to figures 4-33 and 4-34

COEFFICIENTS FOR THE MODEL

E_s	K	C	n	Corr	R_a	R_b
2.023	0.00771	5.803	1.22270	1.39146	0.01540	0.00361

R_a	R_b
0.01540	0.00361

0.6 Amp Discharge

Ah	Volt (Exp)	Volt (Eqn)	Diff
0.00	2.110	2.013	-0.097
1.80	2.050	1.994	-0.056
3.60	2.010	1.970	-0.040
4.20	1.990	1.960	-0.030
4.80	1.970	1.947	-0.023
5.40	1.910	1.925	0.015
5.70	1.880	1.906	0.026
6.00	1.830	1.866	0.036
6.12	1.810	1.833	0.023
6.24	1.770	1.772	0.002
6.30	1.740	1.714	-0.026
6.36	1.690	1.609	-0.081
6.39	1.630	1.514	-0.116
6.42	1.470	1.350	-0.120
6.44	1.030	1.153	0.123

1.5 Amp Discharge

Ah	Volt (Exp)	Volt (Eqn)	Diff
0.00	2.052	2.110	0.058
0.75	2.040	1.991	-0.049
1.50	2.020	1.972	-0.048
2.25	2.000	1.952	-0.048
2.63	1.980	1.942	-0.038
3.00	1.960	1.931	-0.029
3.38	1.940	1.910	-0.030
4.13	1.900	1.868	-0.032
4.50	1.880	1.863	-0.017
4.65	1.850	1.847	-0.003
4.80	1.810	1.825	0.015
4.88	1.770	1.809	0.039
4.95	1.720	1.787	0.067
5.03	1.600	1.754	0.154
5.10	1.100	1.697	0.597
5.13	0.850	1.669	0.819

Numeric Data corresponding to Figures 4-35 and 4-36

Coefficients for the Model

E_s	K	C	n	Corr	R_a	R_b
2.023	0.00771	5.803	1.22270	1.39146	0.01540	0.00361

3.6 Amp Discharge

Ah	Volt (Exp)	Volt (Eqn)	Diff
0.00	2.017	2.002	-0.015
0.30	2.010	1.985	-0.025
0.60	2.000	1.968	-0.032
0.90	1.984	1.950	-0.034
1.20	1.970	1.933	-0.037
1.50	1.960	1.915	-0.045
1.80	1.945	1.897	-0.049
2.10	1.930	1.879	-0.051
2.40	1.910	1.860	-0.050
2.70	1.890	1.840	-0.050
3.00	1.860	1.819	-0.041
3.30	1.830	1.795	-0.035
3.60	1.790	1.766	-0.024
3.78	1.760	1.743	-0.017
3.96	1.710	1.707	-0.003
4.08	1.650	1.665	0.015
4.14	1.590	1.629	0.039
4.20	1.480	1.570	0.090
4.26	1.280	1.446	0.166
4.32	0.940	0.982	0.042

5.4 Amp Discharge

Ah	Volt (Exp)	Volt (Eqn)	Diff
0.00	2.014	1.996	-0.018
0.45	1.980	1.957	-0.023
0.90	1.970	1.919	-0.051
1.35	1.950	1.880	-0.070
1.80	1.920	1.840	-0.080
2.25	1.890	1.799	-0.091
2.70	1.850	1.755	-0.095
3.15	1.800	1.705	-0.095
3.42	1.750	1.665	-0.085
3.60	1.700	1.625	-0.075
3.69	1.660	1.593	-0.067
3.78	1.570	1.540	-0.030
3.87	1.230	1.417	0.187
3.96	0.800	1.109	0.309

0.6A RUN

TYPE OF RUN: DISCHARGE
DATE OF RUN: 05MAY79
BATTERY USED: 6N[illegible]-5BB2
FREQUENCY: 0.0
OPEN CIRCUIT VOLTAGE
STARTING: 2.1[illegible]0
ENDING: 1.9[illegible]0

ELAPSED TIME (MIN)	VOLTAGE (VOLTS)	CURRENT (AMPS)	AMPERE MIN	WATT MIN	TEMP (C)	COMMENTS
0.	2.110	0.60	0.0	0.0	20.0	START OF DISCHARGE
100.	2.060	0.60	100.0	225.2	20.0	
360.	2.010	0.60	216.0	445.0	20.0	
420.	1.990	0.60	252.0	517.0	20.0	
480.	1.970	0.60	288.0	588.2	20.0	
540.	1.910	0.60	324.0	658.1	20.0	
570.	1.860	0.60	342.0	692.2	20.0	
600.	1.850	0.60	360.0	725.6	20.0	
612.	1.810	0.60	367.2	738.7	20.0	
624.	1.770	0.60	374.4	751.6	20.0	
650.	1.740	0.60	378.0	757.9	20.0	
636.	1.650	0.60	381.6	764.1	20.0	
642.	1.620	0.60	385.4	767.1	20.0	
648.	1.470	0.60	388.2	769.6	20.0	
654.	1.920	0.60	392.4	771.5	20.0	START OF DISCHARGE

1.5A RUN

TYPE OF RUN: DISCHARGE
DATE OF RUN: 06MAY79
BATTERY USED: 6N2-5B42
FREQUENCY: 0.0
OPEN CIRCUIT VOLTAGE
STARTING: 2.180
ENDING: 2.000

ELAPSED TIME (MIN)	VOLTAGE (VOLTS)	CURRENT (AMPS)	AMPERE MIN	WATT MIN	TEMP (C)	COMMENTS
0.	2.050	1.50	0.0	0.0	20.0	START OF DISCHARGE
30.	2.040	1.50	45.0	92.7	20.0	
60.	2.020	1.50	90.0	184.1	20.0	
90.	2.000	1.50	135.0	274.5	20.0	
105.	1.990	1.50	157.5	319.4	20.0	
120.	1.980	1.50	180.0	364.1	20.0	
135.	1.970	1.50	202.5	408.8	20.0	
165.	1.910	1.50	247.5	494.4	20.0	
180.	1.880	1.50	270.0	537.1	20.0	
186.	1.840	1.50	279.0	555.8	20.0	
192.	1.810	1.50	288.0	570.7	20.0	
195.	1.770	1.50	292.5	578.2	20.0	
198.	1.720	1.50	297.0	586.1	20.0	
201.	1.600	1.50	301.5	593.0	20.0	
204.	1.100	1.50	306.0	599.7	20.0	
205.	0.000	1.50	307.5	601.2	20.0	END OF DISCHARGE

TYPE OF RUN: DISCHARGE
DATE OF RUN: 05MAY79
BATTERY USED: 6NS-3PM2
FREQUENCY: 0.0
OPEN CIRCUIT VOLTAGE
STARTING: 2.150
ENDING: 2.010

3.6A RUN

ELAPSED TIME (MIN)	VOLTAGE (VOLTS)	CURRENT (AMPS)	AMPERE MIN	WATT MIN	TEMP (C)	COMMENTS
0.	2.000	3.60	0.0	0.0	28.0	START OF DISCHARGE
5.	2.010	3.60	18.0	36.1	28.0	
10.	2.000	3.60	36.0	72.2	28.0	
15.	1.980	3.60	54.0	108.0	28.0	
20.	1.970	3.60	72.0	143.6	28.0	
25.	1.960	3.60	90.0	178.9	28.0	
30.	1.940	3.60	108.0	214.0	28.0	
35.	1.930	3.60	126.0	248.9	28.0	
40.	1.910	3.60	144.0	283.4	28.0	
45.	1.899	3.60	162.0	317.6	28.0	
50.	1.880	3.60	180.0	351.4	28.0	
55.	1.850	3.60	198.0	384.9	28.0	
60.	1.790	3.60	216.0	417.2	28.0	
65.	1.750	3.60	234.0	436.5	28.0	
66.	1.710	3.60	237.6	455.0	28.0	
68.	1.650	3.60	244.8	467.0	28.0	
70.	1.550	3.60	252.0	472.0	28.0	
70.	1.500	3.60	252.0	479.4	28.0	
71.	1.400	3.60	255.6	482.4	28.0	
72.	0.990	3.60	259.2	487.4	28.0	END OF DISCHARGE

5.4A RUN

TYPE OF RUN: DISCHARGE
DATE OF RUN: 05MAY79
BATTERY USED: 6NE-5P#2
FREQUENCY: 0.0
OPEN CIRCUIT VOLTAGE
STARTING: 2.170
ENDING: 2.[illegible]0

ELAPSED TIME (MIN)	VOLTAGE (VOLTS)	CURRENT (AMPS)	AMPERE MIN	WATT MIN	TEMP (C)	COMMENTS
0.	1.990	5.40	0.0	0.0	26.0	START OF DISCHARGE
5.	2.000	5.40	27.0	53.9	26.0	
10.	1.970	5.40	54.0	107.5	28.0	
15.	1.940	5.40	81.0	160.2	28.0	
20.	1.920	5.40	108.0	212.4	28.0	
25.	1.[illegible]	5.40	135.0	263.8	28.0	
30.	1.850	5.40	162.0	314.3	28.0	
35.	1.790	5.40	189.0	363.4	26.0	
38.	1.750	5.40	205.2	392.1	28.0	
40.	1.730	5.40	216.0	410.7	28.0	
41.	1.660	5.40	221.4	419.8	28.0	
42.	1.570	5.40	226.8	428.5	28.0	
43.	1.250	5.40	232.2	436.1	28.0	
44.	0.[illegible]0	5.40	237.6	441.7	28.0	END OF DISCHARGE

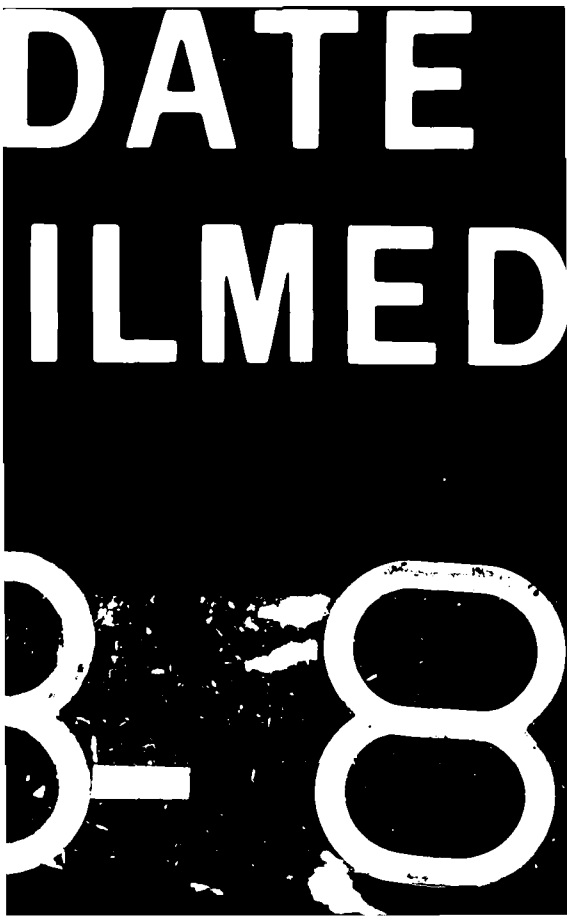
DATE
ILMED
8-8